*Acta Oceanol. Sin.*, 2023, Vol. 42, No. 11, P. 19–34
https://doi.org/10.1007/s13131-023-2168-8
http://www.aosocean.com
E-mail: ocean2@hyxb.org.cn

# Clay minerals and elemental composition of sediments on different sedimentary units in the northern East China Sea shelf: provenance tracing and genetic mechanism analysis

Xiaoyan Xu[1, 4], Yong Zhang[1, 2], Yanguang Dou[1, 3*], Jingyi Cong[1, 3], Beibei Mi[1, 4], Xiaohui Chen[1, 4], Xia Li[1], Chengfen Xu[5], Yongyu Ye[5]

[1] Qingdao Institute of Marine Geology, China Geological Survey, Qingdao 266237, China

[2] Laboratory for Marine Mineral Resource, Pilot National Laboratory for Marine Science and Technology (Qingdao), Qingdao 266237, China

[3] Laboratory for Marine Geology, Pilot National Laboratory for Marine Science and Technology (Qingdao), Qingdao 266237, China

[4] College of Marine Science and Technology, China University of Geosciences (Wuhan), Wuhan 430074, China

[5] Qingdao Marine Geological Engineering Survey Institute Co., Ltd., Qingdao 266071, China

Received 1 November 2022; accepted 5 January 2023

© Chinese Society for Oceanography and Springer-Verlag GmbH Germany, part of Springer Nature 2023

**Abstract**

The composition, provenance, and genetic mechanism of sediment on different sedimentary units of the East China Sea (ECS) shelf are essential for understanding the depositional dynamics environment in the ECS. The sediments in the northern ECS shelf are distributed in a ring-shaped distribution centered on the southwestern Cheju Island Mud. From the inside to the outside, the grain size goes from fine to coarse. Aside from the "grain size effect", hydrodynamic sorting and mineral composition are important restrictions on the content of rare earth elements (REEs). Based on the grain size, REEs, and clay mineral composition of 300 surface sediments, as well as the sedimentary genesis, the northern ECS shelf is divided into three geochemical zones: southwestern Cheju Island Mud Area (Zone Ⅰ), Changjiang Shoal Sand Ridges (Zone Ⅱ-1), Sand Ridges of the East China Sea shelf (Zone Ⅱ-2). The northern ECS shelf is mostly impacted by Chinese mainland rivers (the Changjiang River and Huanghe River), and the provenance and transport mechanism of sediments of different grain sizes is diverse. The bulk sediments come primarily from the Changjiang River, with some material from the Huanghe River carried by the Yellow Sea Coastal Current and the North Jiangsu Coastal Current, and less from Korean rivers. Among them, surface sediments in the southwestern Cheju Island Mud Area (Zone Ⅰ) come mostly from the Changjiang River and partly from the Huanghe River. It was formed by the counterclockwise rotating cold eddies in the northern ECS shelf, which caused the sedimentation and accumulation of the fine-grained sediments of the Changjiang River and the Huanghe River. The Changjiang Shoal Sand Ridges (Zone Ⅱ-1) were developed during the early-middle Holocene sea-level highstand. It is the modern tidal sand ridge sediment formed by intense hydrodynamic action under the influence of the Yellow Sea Coastal Current, North Jiangsu Coastal Current, and Changjiang Diluted Water. The surface sediments mainly originate from the Changjiang River and Huanghe River, with the Changjiang River dominating, and the Korean River (Hanjiang River) influencing just a few stations. Sand Ridges of the East China Sea shelf (Zone Ⅱ-2) are the relict sediments of the paleo-Changjiang River created by sea invasion at the end of the Last Deglaciation in the Epipleistocene. The clay mineral composition of the surface sediments in the study area is just dominated by the Changjiang River, with the North Jiangsu Coastal Current and the Changjiang Diluted Water as the main transporting currents.

**Key words:** the northern East China Sea shelf, rare earth element, clay mineral, provenance, genetic mechanism

**Citation:** Xu Xiaoyan, Zhang Yong, Dou Yanguang, Cong Jingyi, Mi Beibei, Chen Xiaohui, Li Xia, Xu Chengfen, Ye Yongyu. 2023. Clay minerals and elemental composition of sediments on different sedimentary units in the northern East China Sea shelf: provenance tracing and genetic mechanism analysis. Acta Oceanologica Sinica, 42(11): 19–34, doi: 10.1007/s13131-023-2168-8

## 1 Introduction

The East China Sea (ECS) has garnered increasing attention in recent years as a crucial shelf sea on the East Asian continental margin. Since the Late Quaternary, the ECS has been characterized by complicated ocean currents and sediment distribution, sea level changes, high sediment input from terrigenous sediments, and intense land-ocean interactions (Liu et al., 2004; Dou et al., 2011; Niu, 1985; Shi, 2021). The provenance of the ECS shelf has become a hot spot in the marine geological study of marginal seas, especially the contribution of sediments entering the sea from the Chinese-Korean rivers on the ECS shelf and its transport mechanism, which has been a difficult research problem (Choi et al., 2018; Xu et al., 2009a; Yang et al., 2004; Youn et al., 2006). The surrounding ocean circulation is complicated, im-

Foundation item: The National Natural Science Foundation of China under contract Nos 42276084 and 42176078; the Special survey items of the China Geological Survey under contract Nos DD20190205 and DD20221710.
*Corresponding author, E-mail: douyangaung@gmail.com

pacted by the monsoon, terrain, river entrance, external seawater intrusion, tides, and waves, and includes the Kuroshio, Taiwan Warm Current, Yellow Sea Coastal Current, Yellow Sea Warm Current, and Changjiang Diluted Water (Huh and Su, 1999; Huang et al., 2020; Li and Chang, 2009). The Changjiang River, Huanghe River, and Korean rivers (Han River, Keum River, and Yeongsan River) are the most likely provenance, with the Changjiang River and the Huanghe River delivering about $5\times10^8$ t/a and $1\times10^9$ t/a of sediment to the ECS, respectively (Milliman et al., 1985). They have a significant impact on the ECS Shelf's provenance, the formation of muddy sediments, and the marine ecological environment (Yang, 1988).

The sediment types, diverse provenance, and complex sedimentary environments in the northern ECS shelf are ideal for studying land-ocean change, current systems change, material transport, and climate change (Chen et al., 2019; Liu and Li, 2022). It contains three distinct sedimentary units: Changjiang Shoal, southwestern Cheju Island Mud, and the East China Sea shelf tidal sand ridges (Li et al., 2005). While the composition, provenance, and genesis of surface sediments in the ECS's northern shelf have not been thoroughly researched, there is some controversy. Some researchers assume that the majority of the ECS shelf is relict sediments (Liu, 1987), while others argue that it is a modern tidal sand ridge sediment formed by the massive amount of terrestrial material during the Holocene and later modification (Liu et al., 2014; Liu and Xia, 2004). Previous research has shown that the sediments in the southwestern Cheju Island Mud are counterclockwise eddy sediments with material input from the Huanghe River, Changjiang River, and Korean rivers during the Holocene (Liu et al., 2009; Shi, 2012; Youn and Kim, 2011). However, due to the rapid sea level changes and the complex current systems, the provenance and genesis of surface sediments in the ECS's northern shelf are extremely complicated, and no consensus has yet been achieved.

Rare earth elements (REEs) and clay minerals are relatively conservative in sedimentation. They are commonly regarded as trustworthy indicators of sediment provenance, and their composition in sediments may be utilized to identify the provenance of various rivers (Dou et al., 2015b; Koo et al., 2018). The primary variables influencing the sediment composition of Chinese-Korean rivers are differences in source rock composition and chemical weathering (Yang et al., 2002; Hu et al., 2011). The Changjiang River basin's source rocks are complicated, with apparently developing intermediate-acid igneous rocks and strong chemical weathering (Gong et al., 2012, 2013). The Huanghe River basin's source rocks are characterized by yellow earth and significant physical weathering (Chen et al., 1984; Zhang et al., 1990). The geological background of the Changjiang River basin is more complicated than that of the Huanghe River basin, which is dominated by yellow earth. As a result, the elemental content and variation in Changjiang River sediments are substantially greater than in Huanghe River sediments (Fan et al., 2001; Xiong et al., 2003; Yang and Li, 1999a, 1999b). The Korean rivers are dominated by granite and moderate chemical weathering (Lu et al., 2019; Yang et al., 2003b). As a result, REEs and clay mineral compositions of the sediments of the Huang-He, Changjiang, and Korean rivers differ significantly (Choi et al., 2010; Jung et al., 2006; Li et al., 2014; Song and Choi, 2009; Xu et al., 2009a). Due to the different weathering patterns and rock compositions of each river, there are apparent differences in the content of REEs in Chinese-Korean river sediments. It is feasible to distinguish different river sediments and better understand their contributions and transport mechanisms (Dou et al., 2015b; Jung et al., 2006; Xu et al., 2009a; Yang et al., 2004).

In this study, we analyze the material composition characteristics of clay minerals and bulk sediments from 300 surface sediments to identify controlling factors and explore the provenance and genesis mechanisms of sediments from different sedimentary units in the northern ECS shelf.

## 2 Materials and methods

### 2.1 *Research materials*

Based on the 1:250 000 geological survey project in the northern ECS conducted by the Qingdao Institute of Marine Geology of the China Geological Survey, the R/V *Hai Yang Di Zhi Qi Hao* survey vessel collected 300 surface sediments (0–2 cm) as research materials from 2019 to 2021. The distribution of the samples is 30°–32°N, 124.5°–127.5°E, with an area of about 64 000 km$^2$. The current systems around the study area and the specific sampling locations are shown in Fig. 1.

### 2.2 *Experimental methods*

Grain-size determination: 258 sediment samples (Fig. 1) were analyzed using a laser granularity analyzer (model Mastersizer 2000, Malvern, UK), which has a measurement range of 0.02 μm to 2 000 μm with a deviation of <1% and reproducibility: $\Phi_{50}$ <1%. The analytical result interval is $\Phi$0.25, and the sample weight must be greater than 50 g. The overall laser granularity analysis method is used. Individual samples can be combined with sieving analysis and precipitation methods. Then, the sample has been washed with salt, organic matter removal (10% $H_2O_2$), and calcium component removal (dilute hydrochloric acid). The sample is fully dispersed using the feeder's ultrasonic generator and then entered into the laser granularity analyzer for analysis, and then the results are processed. Each grain size parameter was calculated by the method of moments, including the mean grain size and percentage content of each grain class of gravel, sand, silt, and clay. According to the "Specifications for Oceanographic Survey" (GBT 12763.8–2007) and the Udden-Wentworth grade scale is divided into four classes: greater than 2 mm (less than $\Phi$–1) for the gravel; 2–0.063 mm ($\Phi$–1–$\Phi$–4) for the sand; 0.063–0.004 mm ($\Phi$4–$\Phi$8) for the silt; less than 0.004 mm (more than $\Phi$8) for the clay level. Mean Grain Size (Mz) formula: $Mz = (\Phi_{16} + \Phi_{50} + \Phi_{84})/3$ (They represent the particle size of 16%, 50% and 84% on the accumulation curve).

Rare earth elements determination: 258 sediment samples (Fig. 1) were analyzed by Inductively Coupled Plasma Mass Spectrometry (ICP-MS), and 14 rare earth elements (REEs) were tested, including La, Ce, Pr, Nd, Sm, Eu, Gd, Tb, Dy, Ho, Er, Tm, Yb, and Lu. The samples were put in an oven and heated to 105℃ for 12 h before being removed. The sodium oxide solution was added and melted for 10 min in a high-temperature furnace set to 700℃. After cooling, the REEs was extracted with water to form hydroxide precipitation. Triethanolamine was used to mask iron and aluminum. EDTA solution was used to complex calcium and barium, and then filtered. The hydroxide precipitate of REEs was dissolved in 2 mol/dm$^3$ hydrochloric acid, enriched by strong acidic cation exchange resin, then washed with 5 mol/dm$^3$ hydrochloric acid, evaporated the drench solution, fixed the volume and then measured on the machine.

Clay minerals determination: 281 sediment samples (Fig. 1) were analyzed using an X-ray diffractometer (model D/MAX-rB, Rigaku, Japan), and the extraction was referred to the national standard (GB/T 12763.8–2007) "Specification for Oceanographic Survey-Marine Geology and Geophysics Investigation" method.

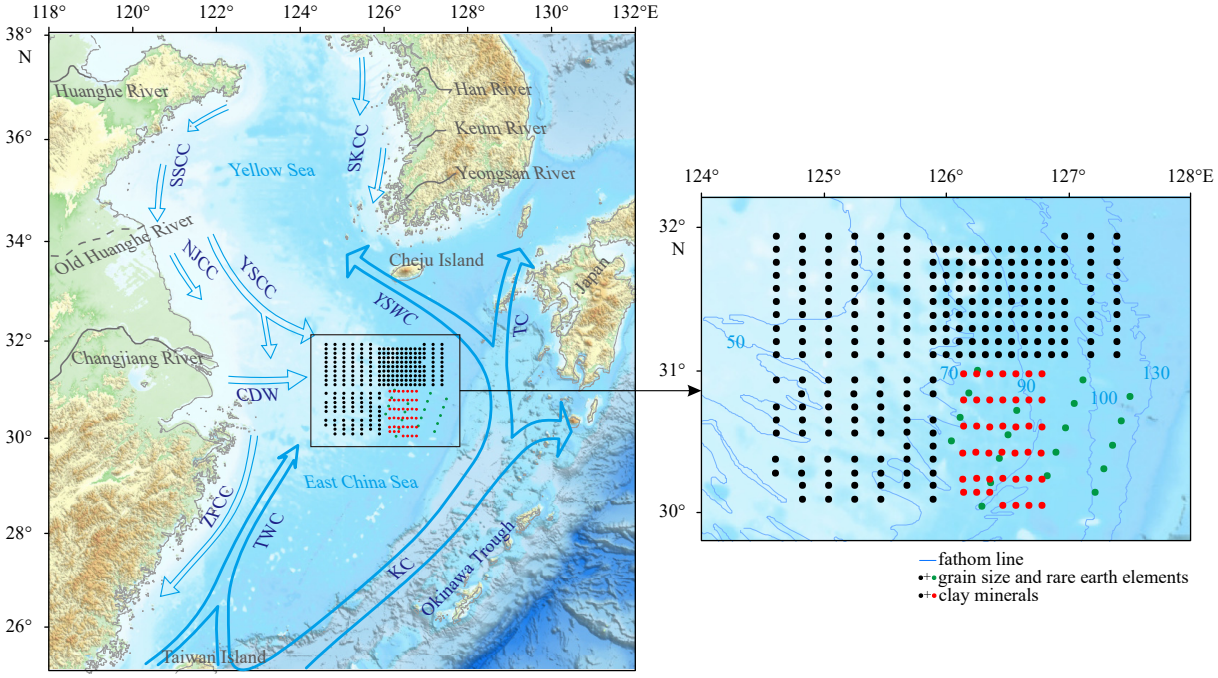


**Fig. 1.** Sampling stations of surface sediments and the current systems in the Northern East China Sea shelf (SSCC: South Shandong Coastal Current; NJCC: North Jiangsu Coastal Current; YSCC: Yellow Sea Coastal Current; CDW: Changjiang Diluted Water; ZFCC: Zhejiang-Fujian Coastal Current; TWC: Taiwan Warm Current; KC: Kuroshio Current; YSWC: Yellow Sea Warm Current; TC: Tsushima Current; SKCC: South Korean Coastal Current. The current systems are modified from Choi et al. (2018) and Dou et al. (2015b)).

The sediment samples were weighed 50–100 g, added with the appropriate amount of hydrogen peroxide to remove organic matter, washed with distilled water, and stirred into a suspension of 1 000 mL. The sediment <0.002 mm particle size was aspirated according to Stokes Law and repeated several times until 5–7 g of dry clay was obtained. The extracted clay fractions were made into ethylene glycol orientation image, natural orientation image, and hydrochloric acid-treated orientation image. Each sample was transferred to two slides by wet smearing. Samples were then airdried prior to XRD analysis. One slide was first measured directly after the air-drying, and then measured again after ethylene-glycol solvation for 48 h. Another slide was heated at 490℃ for 2 h and then analyzed (Liu et al., 2003). The analyses were conducted using a Rigaku D/max-rB X-ray diffractometer (Cu$K\alpha$ radiation, 40 kV voltages; a 100 mA intensity and 2°/min ($2\theta$) speed). The analyses were run from 3° to about 35°($2\theta$). Identification of specific clay minerals was made using the basal layer plus the interlayer revealed by XRD patterns (Brown and Brindley, 1980). Semi-quantitative estimates of peak areas of the basal reflections for the main clay mineral groups of smectite (including mixed-layers) (15–17 Å), illite (10 Å), and kaolinite/chlorite (7 Å) were carried out on the glycolated curve, as it described in detail by Liu et al. (2010). Peak areas were calculated after manual baseline correction using Jade software version 5.0, following the semi-quantitative method of Biscaye (1965), and Biscaye et al. (1997). The error of this method is estimated to be about 8%–10% of the relative abundance of each clay mineral.

The determination of grain size, rare earth elements, and clay mineral content of surface sediments in this study were completed at the Experimental Testing Center of Qingdao Institute of Marine Geology, China Geological Survey.

## 3 Results

### 3.1 *Content and distribution characteristics of grain size*

Table 1 shows the mean, minimum, maximum, and standard deviation coefficients of the grain size fraction and mean grain size of 258 surface sediment samples in the study area. The standard deviation coefficient is the ratio of the standard deviation to the mean and is an important indicator of the degree of data dispersion. The content distribution of each grain size parameter is shown in Fig. 2.

There are only 11 gravel-bearing stations in all, with 10 of them located in the northeast part of the study area and one in the northwest. The total average gravel concentration is 0.26%, while the gravel content of the 11 stations ranges from 0.35% to 33.44%, with a 6.23% average. The sand content ranged from 0.43% to 97.32%, with a 34.26% average. The sand content is lowest in the north-central part of the study area, where it does not exceed 20% and progressively rises to the surrounding area. The highest sand content is located in the southeast, where the content generally exceeds 70%, followed by the southwest, where the

**Table 1.** Grain size composition and parameter characteristics of surface sediments

| Grain size parameters | Mean | Minimum | Maximum | Standard deviation coefficient |
|---|---|---|---|---|
| Gravel content | 0.26% | 0.00% | 33.44% | 8.54 |
| Sand content | 34.26% | 0.43% | 97.32% | 0.03 |
| Silt content | 43.88% | 2.14% | 67.86% | 0.08 |
| Clay content | 21.60% | 0.54% | 36.33% | 0.06 |
| Mean grain size | $\Phi$5.58 | $\Phi$1.14 | $\Phi$7.58 | 0.25 |

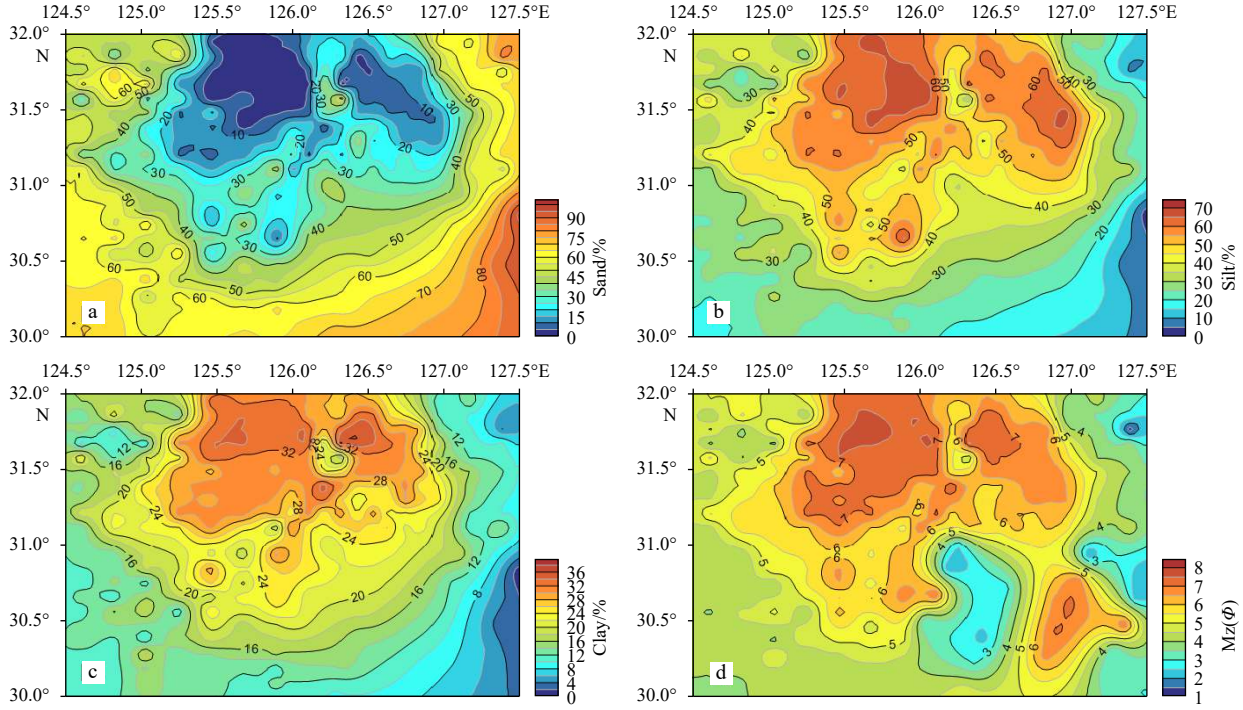


**Fig. 2.** Distribution of different size fractions content and mean grain size in surface sediments in the northern East China Sea shelf (a. sand, b. silt, c. clay and d. mean grain size).

sand content is above 60% (Fig. 2a). Silt content ranges from 2.14% to 67.86%, with an average of 43.88%. Its distribution is opposite to the distribution trend of sand components. The north-central part is the high-value area of silt components, which is generally more than 50%. The lowest value area is located in the southeast, and its content does not exceed 20% (Fig. 2b). The clay content ranges from around 0.54% to 36.33%, with an average of 21.60%. Its distribution is nearly identical to the silt component's distribution trend. The high-value area is located in the study area's north-central region and rapidly diminishes in a circular belt surrounding it. The highest content of clay component is often higher than 27% in the north-central study region, while the lowest content is less than 10% in the southeast corner (Fig. 2c).

The mean grain size varies from $\Phi$1.1 to $\Phi$7.6, with a mean value of $\Phi$5.58. The low-value area is mainly located in the south-central part of the study area. The eastern margin is 120 m deep, and the mean grain size does not exceed $\Phi$4. The sediment type is mainly sand components. In contrast, the high-value area is mainly located in the north-central part, and the mean grain size is above $\Phi$6, and the sediment type in these areas is mainly silt components (Fig. 2d).

The surface sediment types in the study area were mapped according to the Folk's classification (Folk et al., 1970) (Fig. 3). The surface sediments of the northern ECS shelf are divided into two categories: gravel-bearing and non-gravel-bearing sediments. Gravel-bearing sediments are distributed in a small area in the northeast corner of the study area, and also scattered in the northwest corner. And the types can be mainly classified into three types: muddy gravel (mG), gravelly mud (gM), and (gravelly) mud ((g)M). The non-gravel-bearing surface sediments can be divided into 6 types: silt (Z), silty sand (zS), sandy silt (sZ), mud (M), muddy sand (mS), and sandy mud (sM). Their distribution characteristics are described as follows: sandy silt and silty sand with the widest distribution area in the study area, followed by sandy mud and muddy sand, and the two types of mud and silt with relatively small distribution areas. In the north-central part is the muddy area in the southeast of Cheju Island, and the sediment type is mainly silt and mud, and the boundary area is mostly distributed with sandy mud. There are large areas of sandy silt and sandy mud distributed around the muddy area. The eastern and western boundaries are dominated by silty sand, and the southern is mostly distributed with muddy sand. On the whole, the sediment types in the study area are clearly differentiated in a ring-like pattern, from the inner to the outer ring as fine-grained sediment (silt and mud)-coarse and fine mixed (sandy silt and muddy sand)-coarser sediment (silty sand and muddy sand).

### 3.2 *Content and distribution characteristics of REEs*

There are 14 REEs in 258 surface sediments in the study area, including La, Ce, Pr, Nd, Sm, Eu (light rare earth elements, LREEs) and Gd, Tb, Dy, Ho, Er, Tm, Yb, Lu (heavy rare earth elements, HREEs). Table 2 shows the specific content characteristics and main parameters. The total rare earth elements (ΣREE) in the surface sediments of the study area mainly varied between 88.33 μg/g and 261.30 μg/g, with a 163.36 μg/g average, and the ratio of light and heavy rare earth elements (∑LREE/∑HREE) was about 9.64.

The distribution of ΣREE and $\delta$Eu, $(La/Yb)_{UCC}$, $(Gd/Yb)_{UCC}$, $(La/Sm)_{UCC}$, $\delta$Ce normalized by the Upper Continental Crust (UCC) are shown in Fig. 4 (McLennans, 2001). The distribution of ΣREE shows a decreasing trend from west to east, with a high value (>200 μg/g) in the northwestern part and a low value (<125 μg/g) in the northeastern part of the study area (Fig. 4a). The high and low-value areas of $\delta$Eu are blocky distributed. The overall $\delta$Eu is slightly larger than 1.00, ranging from 0.94 to 1.18. It shows a slight positive Eu anomaly (Fig. 4b). The contour distribution maps of $(La/Yb)_{UCC}$ and $(Gd/Yb)_{UCC}$ are similar, with the low-value area appearing in the north-central part and the high-value areas in the south (Fig. 4c, d). The low values of $(La/Sm)_{UCC}$ were

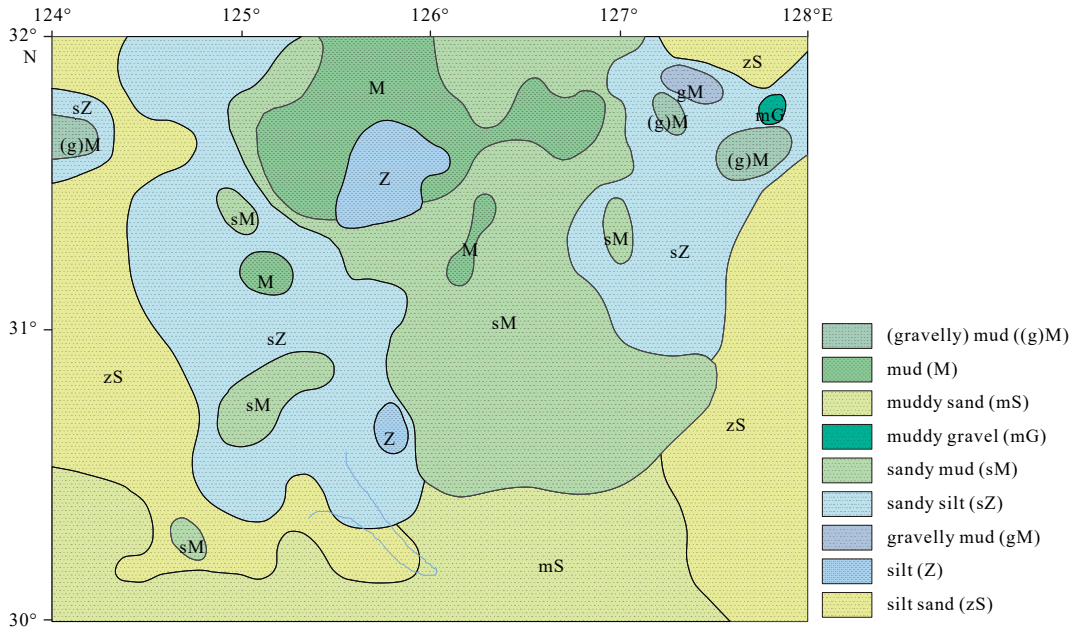


**Fig. 3.** Surface sediment types in the northern East China Sea shelf.

**Table 2.** Characteristics of rare earth element content in surface sediments

| REEs | Mean/ (μg·g$^{-1}$) | Minimum/ (μg·g$^{-1}$) | Maximum/ (μg·g$^{-1}$) | Standard deviation coefficient |
|---|---|---|---|---|
| La | 34.91 | 19.40 | 57.40 | 0.16 |
| Ce | 68.18 | 36.30 | 113.00 | 0.16 |
| Pr | 8.06 | 4.42 | 12.70 | 0.15 |
| Nd | 30.21 | 16.70 | 46.90 | 0.15 |
| Sm | 5.47 | 2.90 | 8.05 | 0.15 |
| Eu | 1.14 | 0.62 | 1.50 | 0.13 |
| Gd | 4.75 | 2.48 | 6.85 | 0.15 |
| Tb | 0.72 | 0.37 | 0.98 | 0.15 |
| Dy | 4.05 | 2.10 | 5.60 | 0.16 |
| Ho | 0.79 | 0.40 | 1.11 | 0.16 |
| Er | 2.24 | 1.18 | 3.40 | 0.17 |
| Tm | 0.34 | 0.18 | 0.47 | 0.17 |
| Yb | 2.17 | 1.10 | 3.11 | 0.17 |
| Lu | 0.34 | 0.18 | 0.48 | 0.17 |
| ∑LREE | 148.14 | 80.34 | 239.55 | 0.16 |
| ∑HREE | 15.41 | 7.99 | 21.75 | 0.15 |
| ∑LREE/ ∑HREE | 9.64 | 8.57 | 11.74 | 0.06 |
| ∑REE | 163.36 | 88.33 | 261.30 | 0.15 |

distributed in the southeast (<3.75), while the other areas showed a blocky distribution with ratios above 3.95 (Fig. 4e). The low values of $\delta$Ce were found in the northeast (<0.91) and the high-alue areas in the southeast (>0.95), showing a trend of gradually decreasing from the southeast to the north. The value of $\delta$Ce ranges from 0.89 to 0.99, indicating a slight negative Ce anomaly (Fig. 4f).

### 3.3 *Content and distribution characteristics of clay minerals*

Four major clay minerals were identified in 281 surface sediments in the study area, and the content characteristics and main parameters are shown in Table 3. There is only one clay mineral combination type (according to the relative content of clay minerals from high to low): illite (61.38%)–chlorite (21.31%)–kaolinite (11.97 %)–smectite (5.35 %).

There are some differences in the spatial distribution of each of the four clay minerals. Illite had the highest percent content, with an average of 61.38% and the largest variation range between 54.76% and 68.98%. The low-value area (<59%) showed a patchy circular distribution, mainly in the western. The high-value area (>65%) is in a blocky distribution in the northeast and southeast central part of the study area (Fig. 5a). Chlorite had the second highest percent content, with an average of 21.31% and a variation range between 17.39% and 25.77%. The low-value area (<19.5%) is mainly in the northwest, and the high-value area (>23.5%) is mainly in the northeast (Fig. 5b). The average percentage of kaolinite is 11.97%, with a range of variation between 7.98% and 15.95%. The low-value area (<11%) is mainly in the east of the study area, and the high-value area (>13%) is in the west (Fig. 5c). The lowest percent smectite content is 5.35% with a range of 1.87%–9.93%, and the high-value area (>7%) is mainly distributed in the northwest, decreasing in a ring around (Fig. 5d). In general, the percentages of illite and chlorite in the study area showed a trend of high in the east and low in the west, while the percentages of kaolinite and smectite, on the contrary, showed a trend of high in the west and low in the east. The smectite/chlorite and kaolinite/illite ratios, their distribution map overall high-value areas and low-value areas are distributed in a block pattern, with high-value areas concentrated in the northwest and low-value areas appearing in the south and east, showing a gradually increasing trend from east to west (Figs 5e, f).

## 4 Discussion

### 4.1 *Grain size control*

Grain size is one of the main properties of sediments. It is an essential basis for classifying sediment types and a reliable indicator of the physical geography and hydrodynamic conditions (Zhao et al., 2021). The grain size composition of sediments is mainly controlled by the composition of their source rocks. Secondly, weathering, mechanical abrasion during transport, hydrodynamic action, and chemical dissolution also have some in-

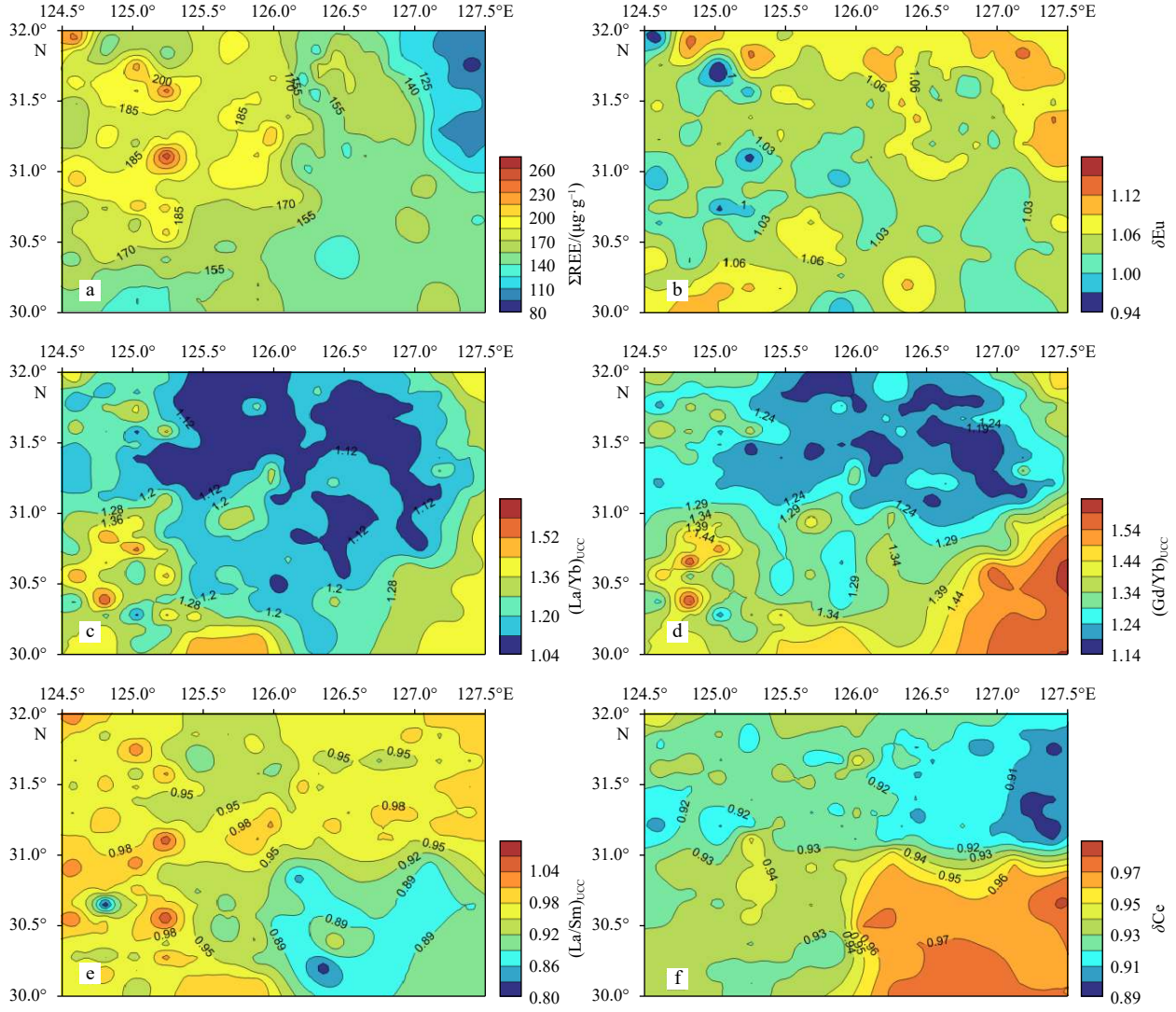


**Fig. 4.** Distribution of REE parameters in surface sediments in the northern East China Sea shelf (a. ΣREE, b. $\delta$Eu, c. $(La/Yb)_{UCC}$, d. $(Gd/Yb)_{UCC}$, e. $(La/Sm)_{UCC}$ and f. $\delta$Ce).

**Table 3.** Characteristics of clay mineral content in surface sediments

| Clay minerals | Mean/% | Minimum/% | Maximum/% | Standard deviation coefficient |
|---|---|---|---|---|
| Illite | 61.38 | 54.76 | 68.98 | 0.04 |
| Chlorite | 21.31 | 17.39 | 25.77 | 0.08 |
| Kaolinite | 11.97 | 7.98 | 15.95 | 0.15 |
| Smectite | 5.35 | 1.87 | 9.93 | 0.31 |

fluence (Zhao et al., 1986). Moreover, the grain size varies in different depositional environments with varied topography, transport media, densities, flow rates, flow directions, and hydrodynamic conditions (McLaren and Bowles, 1985). Based on the grain size characteristics of the sediment, it is possible to trace the provenance of the sediment and the deposition environment and then elucidate the deposition process (Dou et al., 2018; Wang et al., 2020).

Grain size frequently influences the geochemical fraction of sediments in marine settings, and hydrodynamic sorting of sediments can produce chemical differentiation during sediment transport and deposition (Lupker et al., 2013; Wang et al., 2007; Zhao and Yan, 1994). Sediment elemental content varies regularly by grain size composition, i.e., the "grain size effect" of elements (Zhao and Yan, 1994). Therefore, before interpreting the geochemical composition of sediments and exploring the provenance, it is necessary first to consider the effect of removing the grain size effect (Bi et al., 2015). The Late Quaternary land-ocean interactions and environmental changes on the ECS shelf have resulted in a unique sedimentary system with highly variable sediment grain size composition (Dou et al., 2018).

In the northeastern study area, the gravel-bearing area has the lowest mean grain size value, which does not surpass $\Phi$2.5. This area is located at the Late Epipleistocene paleo-shore, and the grain size distribution is primarily influenced by the residual paleo-shore sedimentation. The distribution of gravels and shells in the sediment results in the coarse mean grain size (Li et al., 2005). Since the Holocene sea-level highstand, the north-central

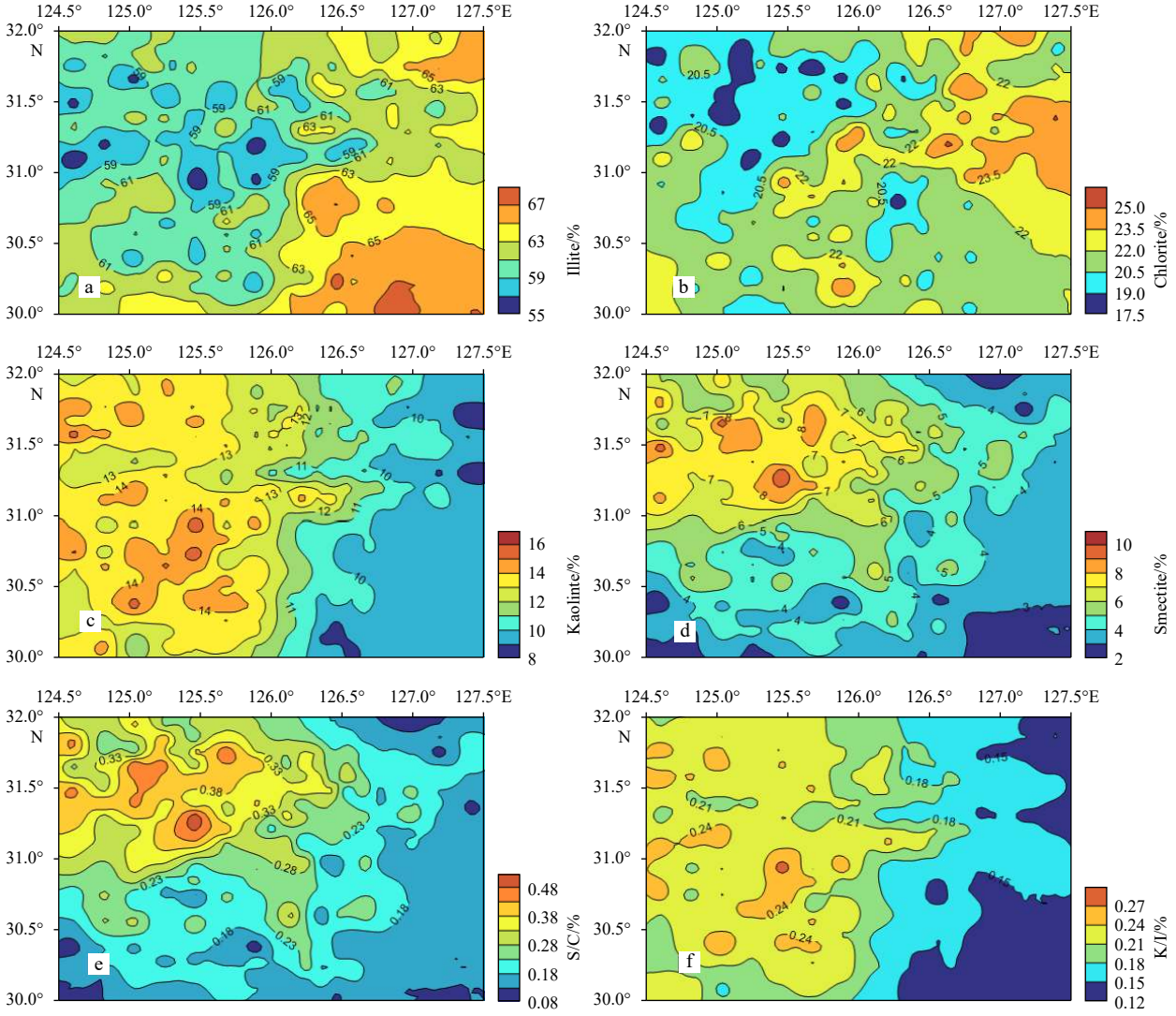


**Fig. 5.** Distribution of clay minerals parameters in surface sediments in the northern East China Sea shelf (a. illite, b. chlorite, c. kaolinite, d. smectite, e. smectite/chlorite and f. kaolinite/illite).

part of the study area has been influenced by the modern circulation system. On the east of the Yellow Sea Warm Current and the Korean Coastal Current, an anticyclonic eddy circulation formed. The suspended sediments of saltwater were irradiated and deposited at the bottom, resulting in the formation of the southwestern Cheju Island Mud, which was dominated by fine-grained particles of silt and clay. It has a mean grain size of $\Phi$6 or more and overlies the Epipleistocene residual sand ridges (Cho et al., 2013; Dou et al., 2015b). Meanwhile, there is no Holocene sediment in the south, and only residual coarse-grained sediments remain (Li et al., 2005).

To investigate the relationship between REEs and grain size, we correlated the REEs and other parameters with the mean grain size ($\Phi$) and the content of sand, silt, and clay (Pearson method). The calculated results were tested by a two-tailed significance test (Table 4). The negative correlation with sand content and the positive correlation with silt and clay imply that REEs are more enriched in fine-grained sediments. It is due to fine-grained muddy sediments made of clay minerals rich in certain compositions such as Mg, Al, Fe, Na, K, mica, illite, chlorite, Fe-hydroxides, and organic matter. Furthermore, they have a considerable adsorption effect on the elements (Du et al., 2003; Qiao and Yang, 2007; Zhao and Yan, 1994).

### 4.2 *Surface sediment provenance analysis*

#### 4.2.1 *Surface sediment zoning*

The content of macronutrients ($SiO_2$, $Al_2O_3$, CaO, MgO, $K_2O$, $Na_2O$, and $TFe_2O_3$), trace elements (Cr, Zn, Cu, Co, Ni, Rb, Zr, Nb, Ti, and Th) and REEs parameters ($\sum$REE, $(Gd/Yb)_{UCC}$, $(La/Sm)_{UCC}$, $(La/Yb)_{UCC}$, $\delta$Eu, and $\delta$Ce) in the sediments were selected to perform Q-type clustering analysis into two categories. The Ward Method was used to calculate the distance using the Square Euclidean distance (SPSS software). Combining the characteristics of topographic and geographic elements in the area, the surface sediments were divided into three geochemical zones: Zone Ⅰ is located in the mud area southwest of the Cheju Island and the surrounding area in the north-central shelf of the ECS; Zone Ⅱ is the tidal sandy sediments of the northern ECS shelf. However, the genesis periods and mechanisms of deposition differ between the east and west. According to the previous study, Zone Ⅱ was divided into two parts with a boundary of 126°E, and the specific distribution and composition characteristics are shown in Fig. 6 and Table 5. Zone Ⅱ-1 is the Changji-

**Table 4.** Correlation of different parameters of REEs and particle size in surface sediments

| | $(La/Yb)_{UCC}$ | $(Gd/Yb)_{UCC}$ | $(La/Sm)_{UCC}$ | $\delta$Ce | $\delta$Eu | ∑LREE | ∑HREE | ∑LREE/∑HREE | ∑REE | Sand | Silt | Clay | Mz |
|---|---|---|---|---|---|---|---|---|---|---|---|---|---|
| $(La/Yb)_{UCC}$ | 1 | | | | | | | | | | | | |
| $(Gd/Yb)_{UCC}$ | 0.883** | 1 | | | | | | | | | | | |
| $(La/Sm)_{UCC}$ | 0.336** | −0.091 | 1 | | | | | | | | | | |
| $\delta$Ce | 0.303** | 0.560** | −0.445** | 1 | | | | | | | | | |
| $\delta$Eu | −0.263** | −0.220** | −0.117 | −0.305** | 1 | | | | | | | | |
| ∑LREE | 0.098 | 0.001 | 0.144* | 0.289** | 0.289** | 1 | | | | | | | |
| ∑HREE | −0.306** | −0.315** | −0.055 | 0.197** | 0.197** | 0.909** | 1 | | | | | | |
| ∑LREE/∑HREE | 0.969** | 0.771** | 0.445** | 0.216** | 0.216** | 0.179** | −0.242** | 1 | | | | | |
| ∑REE | 0.061 | −0.029 | 0.126* | 0.283** | 0.283** | 0.999** | 0.925** | 0.141* | 1 | | | | |
| Sand | 0.723** | 0.755** | 0.075 | 0.280** | 0.280** | −0.337** | −0.609** | 0.645** | −0.366** | 1 | | | |
| Silt | −0.718** | −0.750** | −0.071 | −0.287** | −0.287** | 0.347** | 0.614** | −0.638** | 0.375** | −0.986** | 1 | | |
| Clay | −0.683** | −0.696** | −0.107 | −0.198** | −0.198** | 0.359** | 0.618** | −0.613** | 0.386** | −0.964** | 0.926** | 1 | |
| Mz | −0.579** | −0.585** | −0.085 | −0.179** | −0.179** | 0.385** | 0.610** | −0.531** | 0.410** | −0.860** | 0.858** | 0.857** | 1 |

Note: ** Correlation is significant at the 0.01 level (2-tailed). * Correlation is significant at the 0.05 level (2-tailed).

ang Shoal Sand Ridges, and Zone Ⅱ-2 is the Sand Ridges of the East China Sea shelf (Li et al., 2005). Zone Ⅰ is dominated by fine-grained sediments, with a mean grain size greater than $\Phi$6. Zone Ⅱ is relatively coarse-grained, with an average grain size of less than $\Phi$5. The compositional characteristics of Zone Ⅰ and Zone Ⅱ-1 are similar, and the contents are both characterized by high ΣREE-low illite. In contrast, Zone Ⅱ-2 is characterized by low ΣREE-kaolinite-smectite, with noticeable differences.

It is noteworthy that the REEs content in the southwestern Cheju Island Mud (Zone Ⅰ), which has a finer grain size and more stable hydrodynamic conditions, is expected to be relatively high under the influence of the grain size effect. However, Table 5 shows that the ΣREE content of sediments in Zone Ⅱ-1 is higher than that in Zone Ⅰ. It may be related to the influence of circulation in the YS and ECS, resulting in the flourishing of cold water species under the control of the cold eddies. It would lead to increased biological debris in the sediments and the enhanced dilution of REEs (Ding, 2008; Feng et al., 2011; Wang, 2014). The high value of REEs content in Zone Ⅱ-1, which is distributed in the shallow water depth near the land side (Fig. 4a). It indicates that REEs are continental elements, and the high value may be related to the heavy mineral fraction rich in REEs (Lan et al., 2018; Liu and Li, 2022; Zhang et al., 2016). Zone Ⅱ-2 has few REEs which may be influenced by quartz, with almost no REEs in coarse-grained deposits (Ji, 2003).

#### 4.2.2 *Indication of REEs to provenance in the bulk sediments*

It was found that the main factors affecting the elemental composition and distribution of surface sediments in marine areas are provenance, hydrodynamic environment, water depth, topography, and geomorphology, among which provenance is the primary factor. Furthermore, the regional sediment dynamics conditions are related to sediment redistribution (Wang et al., 2020). The study area is located in the northern ECS shelf, where the surface sediments are mainly from the input of land-based rivers. It means that the sediments are basically of terrestrial origin (Li et al., 2012). REEs are relatively stable in the epigenetic environment, and the composition and distribution of REEs in sedi-

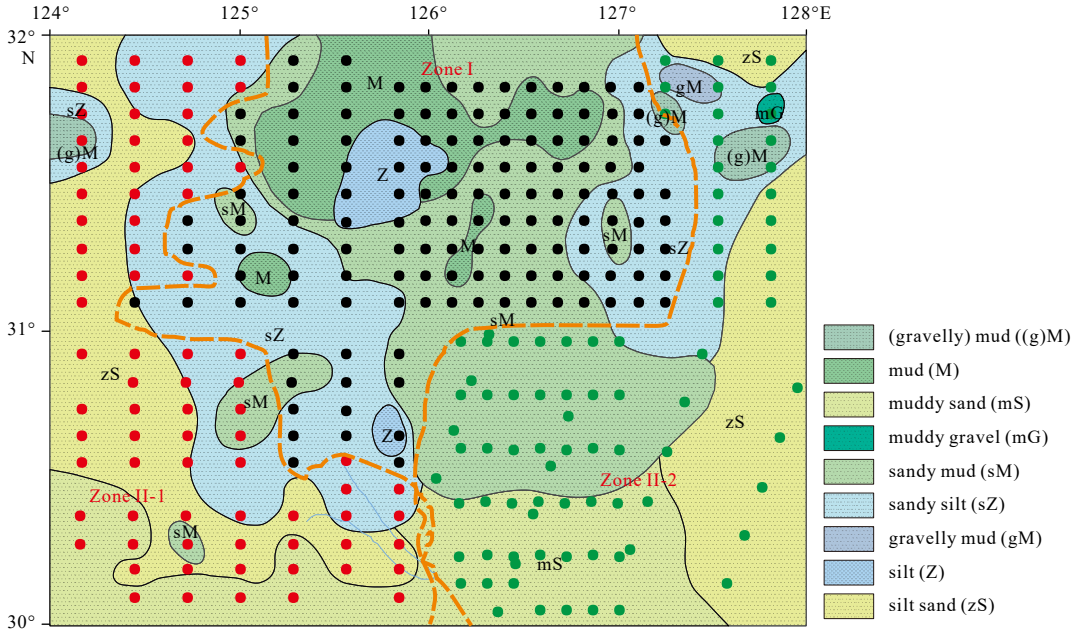


**Fig. 6.** Classification of surface sediments in the northern East China Sea shelf (Zone Ⅰ: southwestern Cheju Island Mud Area; Zone Ⅱ-1: Changjiang Shoal Sand Ridges; Zone Ⅱ-2: Sand Ridges of the East China Sea shelf).

**Table 5.** Compositional characteristics of surface sediments in different regions

| Sediment parameter | Zone Ⅰ | Zone Ⅱ-1 | Zone Ⅱ-2 |
|---|---|---|---|
| Mz($\Phi$) | 6.34 | 4.59 | 4.11 |
| REEs/(μg·g$^{-1}$) | 166.96 | 175.64 | 124.28 |
| Illite/% | 60.73 | 60.38 | 64.32 |
| Chlorite/% | 21.35 | 20.79 | 21.80 |
| Kaolinite/% | 12.13 | 13.36 | 9.87 |
| Smectite/% | 5.79 | 5.46 | 4.01 |

ments depend mainly on the source rocks. It is little affected by weathering, transport, hydrodynamics, sedimentation, diagenesis, and metamorphism. As a result, REEs are frequently utilized as a tracer of sediment provenance (Yang et al., 2003a; Lan et al., 2018). Many scholars have done extensive research on the elemental geochemistry of the Changjiang, Huanghe, and Korean rivers in this field (Han River, Keum River, and Yeongsan River). Furthermore, it is found that the elemental geochemistry of REEs in the sediments of Chinese-Korean rivers is clearly distinct (Jung et al., 2006; Yang and Li, 1999a). So we can use this distinction to determine the different rivers' sediments.

According to Fig. 7, the REEs in bulk sediments of Chinese-Korean rivers exhibits various partitioning patterns after upper continental crust (UCC) standardization (McLennans, 2001). The REEs of bulk sediments from different sedimentary units exhibits comparable distribution patterns, and the distribution curves of Zone Ⅰ and Zone Ⅱ-1 are almost identical. Zone Ⅰ is more abundant in HREEs. And Zone Ⅱ-1 is more enriched in LREEs, which may be related to the high content of heavy minerals (e.g., monazite) that enrich the LREEs (Jung et al., 2006, 2012). It shows that heavy minerals may impact the REEs content in Zone Ⅱ-1. The sediment REEs values of Zone Ⅱ-2 are all less than 1.00 after UCC normalization. In comparison to the UCC, there is a shortfall, and the REEs concentration is low. The three zones have a generally flat UCC normalization pattern, with no obvious difference between LREEs and HREEs. It is comparable to the Changjiang and Huanghe rivers sediments but distinct from the sediments of the Korean rivers (Yang and Li, 1999a). The UCC normalization in the Korean rivers sediments shows LREEs-enriched and HREEs-deficient patterns (Xu et al., 2009a). In addition, the coastal sediments of Cheju Island exhibit strong Eu anomalies that differ greatly from the surface sediments of the study area. Therefore, the surface sediments in the study area are mainly influenced by the Changjiang and Huanghe rivers in China.

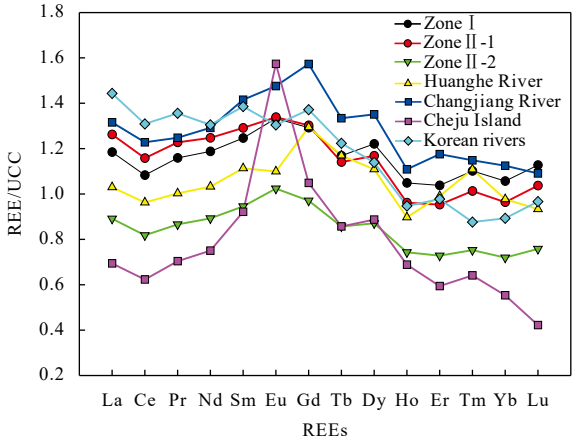


**Fig. 7.** Comparison of UCC normalized distribution curves of surface sediments and potential provenance endmembers (Data of Huanghe River and Changjiang River are from Yang et al. (2002), data of Korean rivers are from Yang et al. (2004), and data of Cheju Island are from Dou et al. (2015b)).

REEs content is susceptible to grain size, and the ratio between REEs can reduce this effect. Based on the REEs data of suspended sediments in Chinese and Korean rivers, it was discovered that Korean rivers sediments (Han River, Keum River, and Yeongsan River) are richer in LREEs compared to Chinese rivers sediments (Changjiang and Huanghe rivers). The ratio of $(La/Yb)_{UCC}$-$(Gd/Yb)_{UCC}$ is markedly different, allowing the provenance of different river sediments to be distinguished (Dou et al., 2015b; Xu et al., 2009a). According to Table 4, $(La/Yb)_{UCC}$ and $(Gd/Yb)_{UCC}$ show a significant correlation with grain size, indicating that the grain size effect may influence them. But the $(La/Sm)_{UCC}$, $\delta$Ce, $\delta$Eu, and ΣREE show a lesser relationship with grain size. The analysis in Section 4.2.1 concluded that, besides the grain size effect, ΣREE content may be influenced by the mineral fraction in the sediment. In addition, there is richer carbonate output in the surface sediments of the ECS. And the negative Ce anomaly is mainly related to authigenic sediments such as biogenic carbonates, which may lead to the inaccuracy of $\delta$Ce discrimination (Zhu et al., 1986; Holser, 1997; Dou et al., 2012). Therefore, $(La/Yb)_{UCC}$-$(Gd/Yb)_{UCC}$ and $(La/Sm)_{UCC}$-$\delta$Eu were chosen to discriminate the sediment provenance (Fig. 8). The discrimination results show that most of the samples in the three zones are close to the Changjiang River sediments. Some of them match the Huanghe River sediments, while just a few samples in Zone Ⅱ-1 are near the Han River. Among them, most of the sediments from the southwestern Cheju Island Mud (Zone Ⅰ) coincide with Changjiang River sediments, and a few are consistent with Huanghe River sediment, indicating that Zone Ⅰ is dominated by Changjiang River. Zone Ⅱ-1 sediments are mainly consistent with the Changjiang River, and only a few stations are consistent with the Korean River. Zone Ⅱ-2 sediments are also dominated by the Changjiang River, and a few stations are consistent with the Huanghe River, which indicates that sand ridges sediments in the Changjiang shoal and the ECS shelf are mainly from the Changjiang River, and just some stations are influenced by the Huanghe River and Korean rivers.

#### 4.2.3 *Indication of clay mineral to the provenance*

The distribution of clay minerals in marine sediments is influenced by the provenance, climatic conditions in the source area, hydrodynamic environment, and geological environment after deposition (Chen, 2008; Han et al., 2022). The formation of authigenic clay minerals requires changes in environmental conditions such as temperature and pressure as the depth of burial increases (Hong, 2010; Zhou et al., 2004). As a result, it is difficult to form authigenic clay minerals in the study area. Clay minerals are mostly terrigenous orogenic clay that is carried into the sea and deposited by weathering. Provenance is the dominant factor controlling the distribution of clay minerals.

Previous studies have shown that the sediments in the Huanghe River, Changjiang River, and Korean rivers have the same clay mineral composition (illite + chlorite + kaolinite + smectite), which is consistent with the results of this study. However, their source rocks and climatic environments are significantly different, resulting in large differences in the content of each clay mineral (Park and Khim, 1992; Fan et al., 2001; Yang et al., 2004; Youn, 2009; Koo et al., 2018). The Changjiang River sediments have high illite (70%), low smectite (5~7%), and illite/

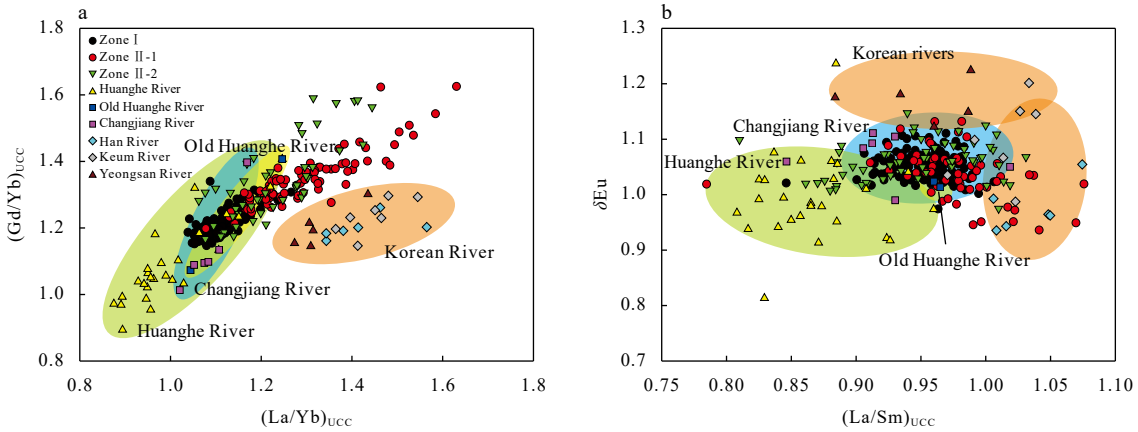


**Fig. 8.** Discrimination maps of REEs in surface sediments (a. $(La/Yb)_{UCC}$-$(Gd/Yb)_{UCC}$, b. $(La/Sm)_{UCC}$-$\delta$Eu. Data of Huanghe River and Changjiang River are from Rao et al. (2017), Xu et al. (2009a), Yang et al. (2004). Data of Old Huanghe River are from Rao et al. (2017). Zhu et al. (2022), and data of Korean rivers are from Xu et al. (2009a)).

smectite >8, whereas the Huanghe River sediments have low illite (60%), high smectite (15%), and illite/smectite <6. As a result, the illite and smectite contents of clay minerals may be used to identify the sediment provenance of the Changjiang and Huanghe rivers. Meanwhile, Korean river sediments have lower smectite (<0.1%) and higher Chlorite and Kaolinite (Chen, 2008; Lan et al., 2011). The smectite-kaolinite-illite+chlorite triangle chart can be used to trace the provenance of Chinese-Korean rivers (Liu et al., 2010, 2007; Liang et al., 2015; Liu, 2010). The smectite/chlorite and kaolinite/illite ratios may also be used to determine distinct provenances by reflecting the degree of weathering of source rocks under different climatic circumstances (Fig. 9) (Liang et al., 2015). The results demonstrate that the Changjiang River is the single provenance of the three sedimentary units, indicating that Changjiang River sediments are more easily transferred into the study area and deposited under the impact of the circulation system.

### 4.3 *Genesis mechanisms of different sedimentary units*

In Section 4.2, the provenance analysis of REEs in the bulk sediments shows that the surface sediments in the study area are mainly mixed Huanghe River and Changjiang River sediments dominated by the Changjiang River. In contrast, the results of clay minerals show that they are mostly Changjiang River sediments. It demonstrates that the surface sediments in the northern ECS shelf are mainly derived from the large amount of land-sourced materials carried by the near-shore water systems in mainland China, such as the Huanghe River and Changjiang River, with the contribution of Korean rivers being very limited. The ECS shelf's complex circulation system and topography, as well as the effect of Quaternary Sea Level Oscillations, have all contributed to the intricacy of shelf sediment generation (Niu, 1985). The contribution and transport mechanisms of potential source rivers in different regions of the northern ECS shelf will be explored by the provenance results and genesis mechanisms of sediments of different grain sizes as follows (Figs 10 and 11).

Southwestern Cheju Island Mud (Zone Ⅰ): The depth range of the southwest Cheju Island Mud is 60–100 m. The seafloor terrain is flat, and diverse water masses meet and mix here, generating a counterclockwise rotating cold vortex (Chen, 2008; Liu et al., 1999). The probability accumulation curves and grain size frequencies of representative stations from three zones were

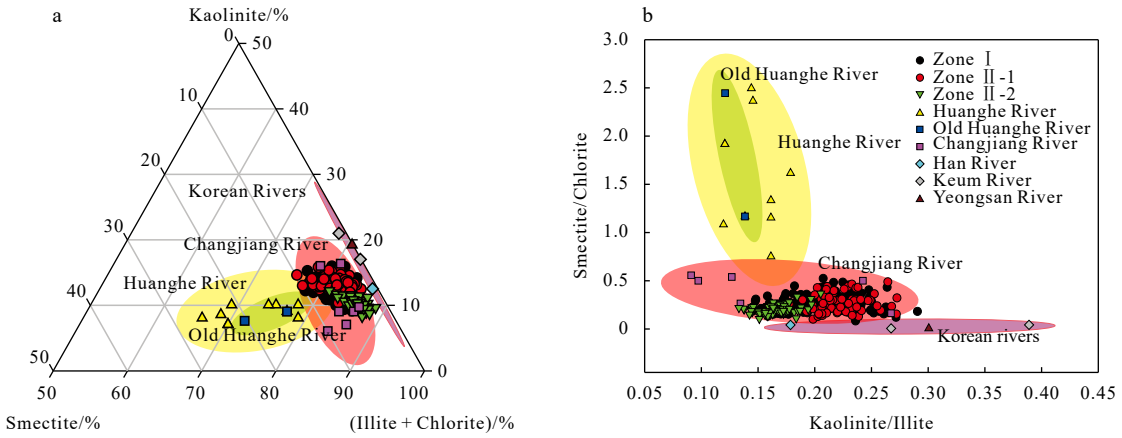


**Fig. 9.** Discrimination map of the source of clay minerals in the surface sediments (a. Smectite-Kaolinite-Illite+Chlorite, b. Smectite/Chlorite-Kaolinite/Illite. Data of Huanghe River are from Lu et al. (2019); Milliman et al. (1985), Park and Khim (1992), Xu et al. (2009b), Yang et al. (2003a), Fan et al. (2001), Ren and Shi (1986), Shi et al. (2019) and Yang (1988). Data of Old Huanghe River are from Lu et al. (2019) and Liang et al. (2015). Data of Changjiang River are from Cho et al. (2015), Choi et al. (2010), Lu et al. (2019), Xu et al. (2009b), Yang et al. (2003b) and Fan et al. (2001). Data of Korean rivers are from Lu et al. (2019) and Park and Khim (1992)).

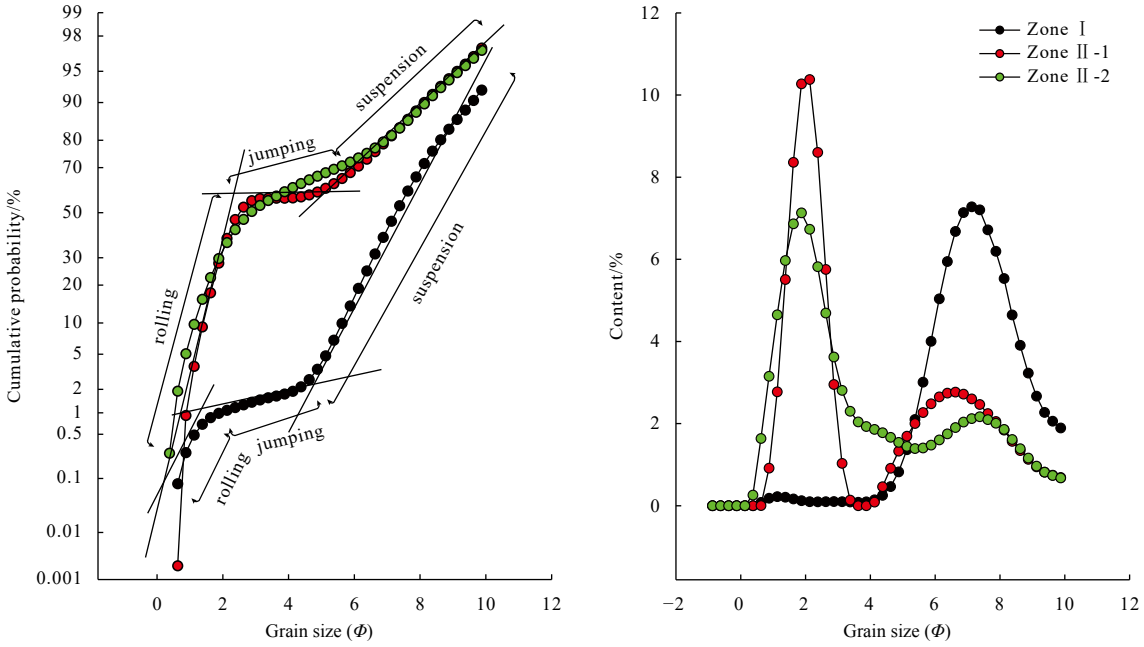


**Fig. 10.** Probability cumulative curve and grain size frequency diagram of surface sediments on the different sedimentary units of study area.

chosen. All three sediment probability accumulation curves show rolling, jumping, and suspension characteristics (Dou et al., 2018; Wang et al., 2012a). Zone Ⅰ has a coarse cut-off point of about $\Phi$1, and the proportion of rolling and jumping components is relatively low. The fine cut-off point is about $\Phi$5, and the proportion of suspended components exceeds 98%. The grain size frequency diagram's positive bias value is skewed toward the fine grain end ($\Phi$6–$\Phi$9) and the frequency curve pattern is asymmetric, with a noticeable fine tail on the left side. It implies that the Southwestern Cheju Island Mud (Zone Ⅰ) is stable and hydrodynamically weak. Under the influence of cold eddy capture with low flow velocity, suspended fine-grained sediments from nearshore rivers settle and collect.

The modern Huanghe River sediments were exported from the Bohai Sea into the YS and transported southward to the northern ECS with the Yellow Sea Coastal Current (Milliman et al., 1985; Guo et al., 1995). In summer, the Changjiang Diluted Water carrying many Changjiang River sediments to the northeast is redirected by the Taiwan Warm Current's top-supporting effect or the induced impact of the YS's cold eddies, and finally also merges into the Yellow Sea Coastal Current (Sun et al., 2000; Zhu et al., 1998; Zhu and Shen, 1997). Moreover, the western branch of the North Jiangsu Coastal Current carries Old Huanghe River Delta material southward. And when it flows through the paleo-Changjiang River Delta, it is joined by a large amount of Changjiang River sediments. Due to the obstruction when passing through the northern Jiangsu Shoal, it is blocked to the southeast and also merges into the Yellow Sea Coastal Current (Dai, 2005; Zhang, 2014). As a result, Zone Ⅰ sediments are characterized by a combination of the Huanghe and Changjiang River. A research found that the sediments in the southwest Cheju Island Mud had been predominantly from the Changjiang River supplied by the Changjiang Diluted Water or Yellow Sea Warm Current for 6 000 years, based on the REEs and clay mineral compositions of three cores (Koo et al., 2021). According to our findings, the surface sediments in the southwestern Cheju Island Mud are mostly impacted by the Changjiang River sediments delivered by the North Jiangsu Coastal Current and the Changjiang Diluted Water. The bulk sediments are a combination of the Huanghe River and Changjiang River, although mainly from the Changjiang River. Furthermore, the clay mineral composition is mainly from the Changjiang River.

Tidal Sand Ridges (Zone Ⅱ): Tidal Sand Ridge is a type of sediment developed from the sea invasion system. The sea invasion system was formed at the isochronous surface during the lowest sea level in the last ice age. The sea invasion layer was deposited from the shelf slope to land with the process of sea invasion, and the bottom surface of its sedimentary layer was diachronism. With the process of sea invasion, the sea level rose in a step-like manner. During the sea level rises gently or stagnantly, large-scale tidal sand ridges are developed. In the rapid sea level rise, there is a "leap" of sand ridge deposition area to shallow water with time evolution. And a new Tidal Sand Ridge will be formed in the new sea level stagnation period. Subsequently, the ECS has formed three phases of tidal sand ridges since the last deglacial period (Li et al., 2005; Yang et al., 2001; Yin, 2003). Among them, the Sand Ridges of the ECS shelf (Zone Ⅱ-2) belong to the first phase of the tidal sandy ridges, which developed at the end of the Last Deglaciation in the Epipleistocene. The Changjiang Shoal Sand Ridges (Zone Ⅱ-1) belong to the second phase of the tidal sandy ridges, which developed in the early-middle Holocene (Li et al., 2005). The sediment probability accumulation curves are similar for the two stations in Zone Ⅱ. The coarse cut-off point is about $\Phi$2, and the fine cut-off point is about $\Phi$5. The proportion of jumping components is quite low while rolling and suspension components are dominating, accounting for about 50% each. Their grain size frequency curves are asymmetric, having double peaks. The major peak is sharp, with positive skewed values toward the coarse end ($\Phi$2). The secondary peak is weak, and the positive skewed values are biased toward the finer end ($\Phi$6–$\Phi$7). It indicates that the sedimentary environment in the sandy area of the Changjiang Shoal Sand Ridges and the Sand Ridges of the ECS shelf is complicated, changeable, and hydrodynamic. Under the action of various circulations, sediments are

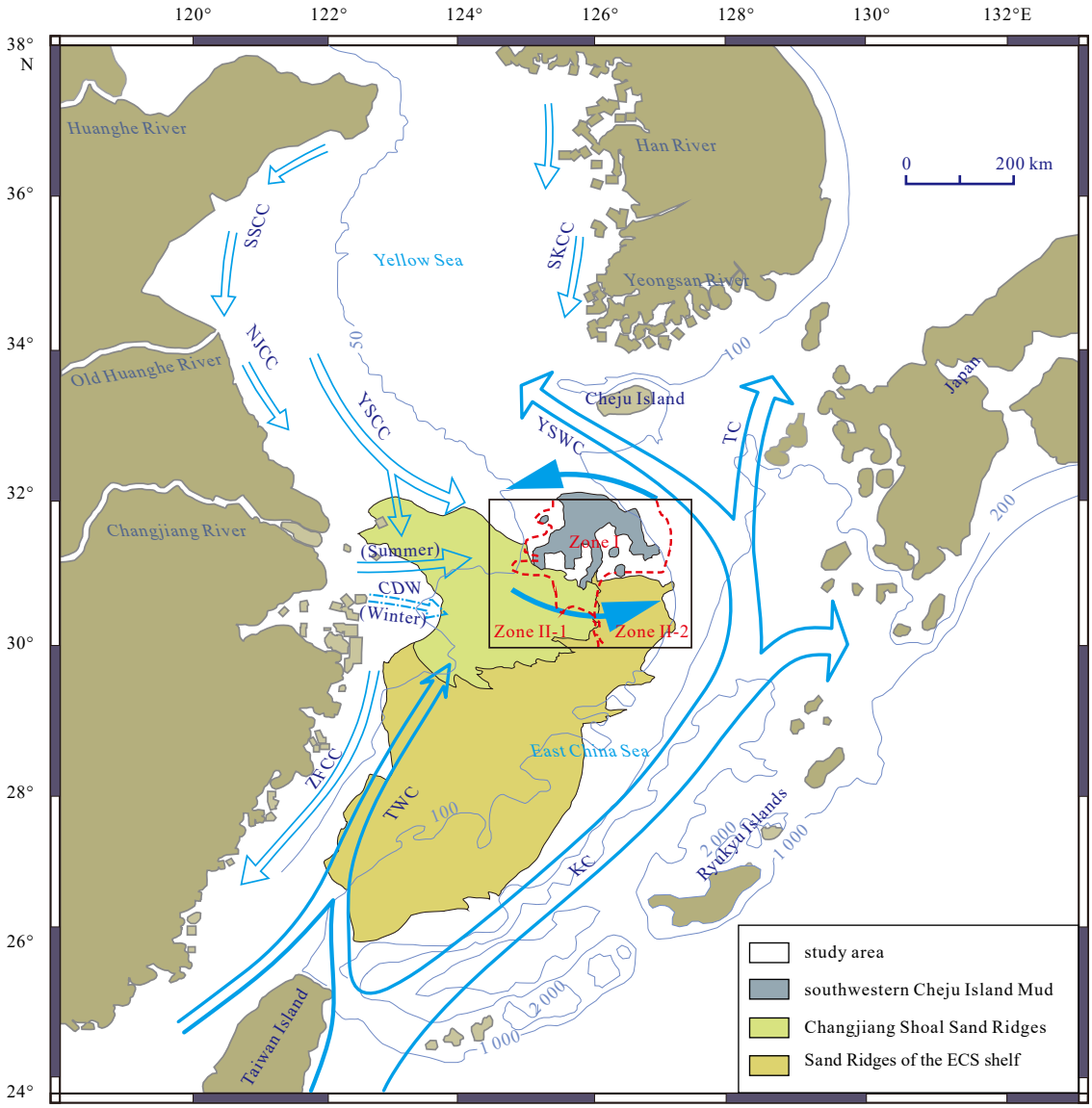


**Fig. 11.** Current systems, study area and sediment transport mechanism of different sedimentary units in the northern East China Sea shelf (Dou et al., 2015a; Li et al., 2005, 2012). (SSCC: South Shandong Coastal Current; NJCC: North Jiangsu Coastal Current; YSCC: Yellow Sea Coastal Current; CDW: Changjiang Diluted Water; ZFCC: Zhejiang-Fujian Coastal Current; TWC: Taiwan Warm Current; KC: Kuroshio Current; YSWC: Yellow Sea Warm Current; TC: Tsushima Current; SKCC: South Korean Coastal Current. The current systems are modified from Choi et al. (2018) and Dou et al. (2015b)).

deposited in the form of rolling coarse particles and suspended fine particles.

Although the Tidal Sand Ridges (Zone Ⅱ) are all sandy deposits, the Changjiang Shoal Sand Ridges (Zone Ⅱ-1) and Sand Ridges of the ECS shelf (Zone Ⅱ-2) have different sediment ages and genesis mechanisms (Liu, 1987； Li et al., 2005). According to the previous study, Zone Ⅱ was divided by 126°E (Li et al., 2005). Most of the area of Zone Ⅱ-2 is located within the geomorphology of the paleo-tidal sand ridges. The sea level during the Last Glaciation was 120–140 m lower than the present. In the early stage, terrestrial rivers carried massive materials into the sea, forming sandy sediments in the coastal sedimentary environment. Then, they were transformed into mat-like sands by sea invasion during the Last Deglaciation in the Epipleistocene and belonged to the "relict sediments" in the paleo-coastal sedimentary environment (Dou et al., 2018; Liu et al., 2014; Liu and Xia, 2004). Due to the blockage of the Taiwan Warm Current and the Kuroshio Current, sediments from China mainland's and Taiwan Island rivers have been difficult to spread to the eastern offshore shelf since the Holocene sea-level highstand. Thus, these early "relict sediments" cannot be covered by modern fine-grained sediments and remain on the seafloor until now (Dou et al., 2018; Wang et al., 2012b). Subsequently, the high sea level stagnated in the early-middle Holocene, and the second phase of the tidal sand ridge, including the Changjiang Shoal Sand Ridges (Zone Ⅱ-1), developed (Li et al., 2005). Zone Ⅱ-1 is mainly distributed in the north of 30°N and between 123°–126°E outside the mouth of the Changjiang River, with a water depth range of 40–80 m. The seafloor in this area is flat and open, with abundant sandy material sources. There is still controversy about its genesis. Earlier studies regarded the Changjiang Shoal as residual shelf deposits or paleo-Changjiang River underwater deltaic deposits (Liu, 1987; Qin et al., 1987). However, based on the tidal action, micro-geomorphology, sediment composition, Holocene sedi-

ment thickness, and foraminiferal composition, it is now generally considered to be a typical modern Tidal Sand Ridge deposit developed in the early-middle Holocene (Liu and Xia, 2004; Wang et al., 2012a). It is affected by strong and complicated hydrodynamic sedimentation. In addition to the reciprocal sorting of tidal currents and storm surges, there are also North Jiangsu Coastal Current, Zhejiang-Fujian Coastal Current, Changjiang Diluted Water, Taiwan Warm Current, and cyclonic eddies in the northern ECS. Various currents and tides act simultaneously, and the seafloor develops widely distributed ripple marks (Wang et al., 2012a, 2020; Ye et al., 2004).

The surface sediments of the tidal sand ridges in the northern ECS shelf are mainly local and nearby shelf sediments. Under the joint action of the Yellow Sea Coastal Current, the North Jiangsu Coastal Current, and the Changjiang Diluted Water, it is also a combination of Huanghe River-Changjiang River sediments, which is greatly affected by the Changjiang River. The ECS shelf has a flat topography, frequent hydrodynamic changes, and is susceptible to sea level fluctuations, so the sedimentary environment is complex and variable. Thus, the sediments are strongly multi-sourced (Wang et al., 2020). Some studies show that the sediments in the YS and ECS shelves have prominent characteristics of "summer storage and winter transport" under monsoon impact (Wang et al., 2020). The Yellow Sea Coastal Current flows southward to transport the modern Huanghe River sediments into the northern ECS (Milliman et al., 1985). Aside from the southeasterly deflection of the North Jiangsu Coastal Current into the tributaries of the Yellow Sea Coastal Current, another branch continues to flow southward across the northern Jiangsu Province. Then the sediments from the Old Huanghe River Delta and the paleo-Changjiang River Delta were also transported southward to the northern ECS (Lu et al., 2019). In summer, the Changjiang Diluted Water usually flows northeastward. Therefore, it is difficult for the Changjiang River sediments carried by the Changjiang Diluted Water and the Changjiang River sediments in the southwest Cheju Island Mud to spread further southward (Cho et al., 2013). However, in winter, the Changjiang Diluted Water also expands to the southeast under the control of the north wind, causing many Changjiang River sediments to reach the Tidal Sand Ridges in the ECS (Zhu and Shen, 1997). The modern Changjiang and paleo-Changjiang River sediments composition is basically the same (Chen, 2008). Combined with the discussion in Section 4.2, it is suggested that the surface sediments in the Changjiang Shoal Sand Ridges (Zone Ⅱ-1) are dominated by the Huanghe River-Changjiang River mixture influenced by the North Jiangsu Coastal Current and the Changjiang Diluted Water. Moreover, it may also be impacted by the Han River, which is transported northwest of the ECS by the South Korean Coastal Current. And the Sand Ridges of the ECS shelf (Zone Ⅱ-2) are relict sediments in the Late Pleistocene that receives almost no modern material. It is mainly a former deposit of the paleo-Changjiang River Delta (Huang et al., 2012; Ning et al., 2022). A few stations may be influenced by the Huanghe River sediments of the Yellow Sea Coastal Current and the North Jiangsu Coastal Current.

## 5 Conclusions

In order to investigate the composition, provenance, and genesis mechanism of bulk sediments and clay grain level sediments in the northern ECS shelf, this study systematically analyzed 300 surface sediments for grain size, REEs, and clay minerals and obtained the following understanding.

(1) The overall sediment type of the surface sediments in the study area is distributed in a circular belt, with the grain size changing from fine to coarse from inside to outside, centered on the southwestern Cheju Island Mud. The content of REEs is governed by other factors, such as hydrodynamic sorting and mineral composition. The northern ECS shelf can be divided into three zones based on the REEs in bulk sediments: The southwestern Cheju Island Mud (Zone Ⅰ), the southwest Cheju Island muddy and the surrounding area, is dominated by fine-grained deposits such as clay and silt. Zone Ⅱ is the tidal sandy sediments of the ECS shelf, of which the Changjiang Shoal Sand Ridges (Zone Ⅱ-1) developed in the early-middle Holocene to the west of 126°E, and to the east is the Sand Ridges of the ECS shelf (Zone Ⅱ-2) developed at the end of the Last Deglaciation in the Epipleistocene.

(2) The provenance and transport mechanisms of sediments of different grain sizes in the study area are different. The bulk sediments are mainly from the Changjiang River sediments, and partly from the Huanghe River sediments under the joint action of the Yellow Sea Coastal Current, North Jiangsu Coastal Current, and Changjiang Diluted Water. Among them, the surface sediments of the southwestern Cheju Island Mud (Zone Ⅰ) come mostly from the Changjiang River and partly from the Huanghe River. It is formed by the counterclockwise rotating cold vortex formed by the meeting and mixing of the water masses such as the North Jiangsu Coastal Current and Changjiang Diluted Water, and the fine-grained sediments of the Changjiang and Huanghe rivers sediments carried by them are deposited and accumulated.

(3) The Changjiang Shoal Sand Ridges (Zone Ⅱ-1) are under the influence of the Huanghe River Coastal Current, the southward North Jiangsu Coastal Current, and the southeastward Changjiang Diluted Water, and the surface sediments are the combination of the Changjiang and Huanghe rivers sediments, but dominated by the Changjiang River. Only a few stations are influenced by the Korean River (Han River). Zone Ⅱ-1 was developed in the early-middle Holocene sea-level highstand. It was influenced by tidal currents, storm surges, and various current systems with abundant sandy material sources. In this way, typical modern tidal sand ridge deposits are formed due to the stronger hydrodynamic sedimentation sorting effect.

(4) The Sand Ridges of the ECS shelf (Zone Ⅱ-2) were relict sediments of the paleo-Changjiang River developed by sea invasion effects at the end of the Last Deglaciation in the Epipleistocene. This area has strong hydrodynamics and has been modified by currents, waves, and other marine dynamics. A few stations may be influenced by the Huanghe River sediments of the Yellow Sea Coastal Current and the North Jiangsu Coastal Current. In contrast, the Changjiang River sediments dominate the clay mineral composition in the northern ECS shelf, and it is mostly carried by the North Jiangsu Coastal Current and the Changjiang Diluted Water.

***Acknowledgements***

We are grateful to the East China Sea expedition led by the CGS (China Geological Survey) for sampling.

## References

Bi Lei, Yang Shouye, Li Chao, et al. 2015. Geochemistry of river-borne clays entering the East China Sea indicates two contrasting types of weathering and sediment transport processes. Geochemistry, Geophysics, Geosystems, 16(9): 3034–3052

Biscaye P E. 1965. Mineralogy and sedimentation of recent deep-sea clay in the Atlantic Ocean and adjacent seas and oceans. GSA Bulletin, 76(7): 803–832, doi: 10.1130/0016-7606(1965)76[803:

MASORD]2.0.CO;2
Biscaye P E, Grousset F E, Revel M, et al. 1997. Asian provenance of glacial dust (stage 2) in the Greenland Ice Sheet Project 2 Ice Core, Summit, Greenland. Journal of Geophysical Research: Oceans, 102(C12): 26765–26781, doi: 10.1029/97JC01249
Brown G, Brindley G W. 1980. X-ray diffraction procedures for clay mineral identification. In: Brindley G W, Brown G, eds. Crystal Structures of Clay Minerals and Their X-ray Identification. London: Mineralogical Society of Great Britain and Ireland Mineralogical Society Monograph, 305–359
Chen Lirong. 2008. Sedimentary Mineralogy of the China Sea (in Chinese). Beijing: China Ocean Press, 121–155, 476
Chen Jingsheng, Li Yuanhui, Le Jiaxiang, et al. 1984. Physical and chemical erosions of rivers in China. Chinese Science Bulletin, 29(15): 932–936, doi: 10.1360/csb1984-29-15-932
Chen Shanshan, Wang Zhongbo, Lu Kai, et al. 2019. Sedimentary stratigraphic framework and palaeoenvironmental evolution of the northern outer shelf of East China Sea since MIS 6. Marine Geology & Quaternary Geology (in Chinese), 39(6): 124–137
Cho H G, Kim S O, Kwak K, et al. 2015. Clay mineral distribution and provenance in the Heuksan mud belt, Yellow Sea. Geo-Marine Letters, 35(6): 411–419, doi: 10.1007/s00367-015-0417-3
Cho H G, Yi H I, Lee Y J, et al. 2013. Clay mineral distribution in the southwestern Cheju island mud. In: Proceedings of 13th International Multidisciplinary Scientific Geo Conference and EXPO SGEM 2013 Water Resources, Forest, Marine and Ocean Ecosystems. Albena, Bulgaria: 815–822
Choi J Y, Koo H J, Cho H G. 2018. Provenance study of 99MAP-P63 core sediments in the East China Sea. Journal of the Mineralogical Society of Korea (in Korean), 31(4): 257–266, doi: 10.9727/jmsk.2018.31.4.257
Choi J Y, Lim D I, Park C H, et al. 2010. Characteristics of clay mineral compositions in river sediments around the Yellow Sea and its application to the provenance of the continental shelf mud deposit. Journal of the Geological Society of Korea (in Korean), 46(5): 497–509
Dai Huimin. 2005. Study on geochemistry characteristics and sources in the mud area southwest of Cheju Island (in Chinese) [dissertation]. Qingdao: Ocean University of China
Ding Ling. 2008. Phytoplankton biomarker ratios in suspended particles from the continental shelf of the East China Sea and reconstruction of the ecosystem structure for mud area in the southwest of Jizhou Island (in Chinese)[dissertation]. Qingdao: Ocean University of China
Dou Yanguang, Chen Xiaohui, Li Jun, et al. 2018. Origin and provenance of the surficial sediments in the subenvironments of the East China Sea. Marine Geology & Quaternary Geology (in Chinese), 38(4): 21–31
Dou Yanguang, Li Jun, Li Yan. 2012. Rare earth element compositions and provenance implication of surface sediments in the eastern Beibu Gulf. Geochimica (in Chinese), 41(2): 147–157
Dou Yanguang, Yang Shouye, Li Chao, et al. 2015a. Deepwater redox changes in the southern Okinawa Trough since the last glacial maximum. Progress in Oceanography, 135: 77–90, doi: 10.1016/j.pocean.2015.04.007
Dou Yanguang, Yang Shouye, Lim D I, et al. 2015b. Provenance discrimination of last deglacial and Holocene sediments in the southwest of Cheju Island, East China Sea. Palaeogeography, Palaeoclimatology, Palaeoecology, 422: 25–35
Dou Yanguang, Yang Shouye, Tang Min, et al. 2011. Using biogenic components to decipher the terrigenous input and paleoenvironmental changes over the last 28ka in the middle Okinawa Trough. Quaternary Sciences (in Chinese), 31(2): 236–243
Du Dewen, Shi Xuefa, Meng Xianwei, et al. 2003. Geochemical granularity effect of sediment in the Yellow Sea. Advances in Marine Science (in Chinese), 21(1): 78–82
Fan Dejiang, Yang Zuosheng, Mao Deng, et al. 2001. Clay minerals and geochemistry of the sediments from the Yangtze and Yellow Rivers. Marine Geology & Quaternary Geology (in Chinese), 21(4): 7–12
Feng Xuwen, Shi Xuefa, Huang Yongxiang, et al. 2011. Distributions and main controlling factors of rare earth elements in core sediments from the Changjiang Estuary mud area over the last 100 years. Geochimica (in Chinese), 40(5): 464–472
Folk R L, Andrews P B, Lewis D W. 1970. Detrital sedimentary rock classification and nomenclature for use in New Zealand. New Zealand Journal of Geology and Geophysics, 13(4): 937–968, doi: 10.1080/00288306.1970.10418211
Gong Chuandong, Dai Huimin, Yang Zuosheng, et al. 2012. Study of granularity effects of rare earth elements in the sediments of Yangtze River. Journal of Geology (in Chinese), 36(4): 349–354
Gong Chuandong, Dai Huimin, Yang Zuosheng. 2013. Comparison of REE variations with grain sizes in sediments between the Yangtze River and the Yellow River. Geology and Resources (in Chinese), 22(2): 148–154
Guo Zhigang, Yang Zuosheng, Wang Zhaoxiang. 1995. Influence of water masses on the distribution of sea-floor sediments in the Huanghai Sea and the East China Sea. Journal of Ocean University of Qingdao (in Chinese), 25(1): 75–84
Han Zongzhu, Wang Yibing, Sun Yuangao, et al. 2022. Composition of minerals in surface sediments of the Yellow Sea and their provenance. Marine Geology Frontiers (in Chinese), 38(4): 10–19
Holser W T. 1997. Evaluation of the application of rare-earth elements to paleoceanography. Palaeogeography, Palaeoclimatology, Palaeoecology, 132(1–4): 309–323
Hong Hanlie. 2010. A review on paleoclimate interpretation of clay minerals. Geological Science and Technology Informatio (in Chinese), 29(1): 1–8
Hu Bangqi, Li Jun, Li Guogang, et al. 2011. Distinguishing the Changjiang and Huanghe sediments: a review. Marine Geology & Quaternary Geology (in Chinese), 31(6): 147–156
Huang Long, Wang Zhongbo, Geng Wei, et al. 2020. Sources and transport of clay minerals in surface sediments of the northeastern East China Sea. Earth Science (in Chinese), 45(7): 2722–2734
Huh C A, Su C C. 1999. Sedimentation dynamics in the East China Sea elucidated from $^{210}$Pb, $^{137}$Cs and $^{239,240}$Pu. Marine Geology, 160(1–2): 183–196, doi: 10.1016/S0025-3227(99)00020-1
Ji Fuwu. 2003. REE Characteristics of core Q43 sediments from outer-shelf of East China Sea and the provenance indicating (in Chinese)[dissertation]. Qingdao: Ocean University of China
Jung H S, Lim D, Choi J Y, et al. 2012. Rare earth element compositions of core sediments from the shelf of the South Sea, Korea: their controls and origins. Continental Shelf Research, 48: 75–86, doi: 10.1016/j.csr.2012.08.008
Jung H S, Lim D I, Yang S Y, et al. 2006. Constraints of REE distribution patterns in core sediments and their provenance, northern East China Sea. Economic and Environmental Geology (in Korean), 39(1): 39–51
Koo H J, Choi J Y, Cho H G. 2021. Provenance change of fine-grained sediments in the South West Cheju Island Mud (SWCIM) since the last glacial period. Journal of the Geological Society of Korea (in Korean), 57(2): 165–179, doi: 10.14770/jgsk.2021.57.2.165
Koo H, Lee Y, Kim S, et al. 2018. Clay mineral distribution and provenance in surface sediments of Central Yellow Sea Mud. Geosciences Journal, 22(6): 989–1000, doi: 10.1007/s12303-018-0019-y
Lan Xianhong, Xu Xiaoda, Wang Zhongbo, et al. 2018. Distribution characteristics of rare earth elements and their provenance constraints in the surface sediments from the Western Bohai Sea. Acta Geoscientica Sinica (in Chinese), 39(1): 37–44
Lan Xianhong, Zhang Xianjun, Liu Xinbo, et al. 2011. Distribution pattern of clay minerals in surface sediments of South Yellow Sea and their provenance. Marine Geology & Quaternary Geology (in Chinese), 31(3): 11–16
Li Tiegang, Chang Fengming. 2009. Paleoceanography in the Okinawa Trough (in Chinese). Beijing: China Ocean Press, 1–259
Li Jun, Hu Bangqi, Dou Yanguang, et al. 2012. Modern sedimentation rate, budget and supply of the muddy deposits in the East China Sea. Geological Review (in Chinese), 58(4): 745–756

Li Jun, Hu Bangqi, Wei Helong, et al. 2014. Provenance variations in the Holocene deposits from the southern Yellow Sea: clay mineralogy evidence. Continental Shelf Research, 90: 41–51, doi: 10.1016/j.csr.2014.05.001

Li Guangxue, Yang Zigeng, Liu Yong. 2005. Origins of Seafloor Sedimentary Environments in Eastern China Sea Regions (in Chinese). Beijing: Science Press, 9–13

Liang Xiaolong, Yang Shouye, Yin Ping, et al. 2015. Distribution of clay mineral assemblages in the rivers entering Yellow Sea and East China Sea and the muddy shelve deposits and control factors. Marine Geology & Quaternary Geology (in Chinese), 35(6): 1–15

Liu Xiqing. 1987. Relict sediments in China continental shelf. Marine Geology & Quaternary Geology (in Chinese), 7(1): 1–14

Liu Zhifei. 2010. Clay mineral assemblages in sediments of the South China Sea: East Asian monsoon evolution proxies. Acta Sedimentologica Sinica (in Chinese), 28(5): 1012–1019

Liu Zhifei, Colin C, Li Xiajing, et al. 2010. Clay mineral distribution in surface sediments of the northeastern South China Sea and surrounding fluvial drainage basins: source and transport. Marine Geology, 277(1–4): 48–60, doi: 10.1016/j.margeo.2010.08.010

Liu Yong, Li Guangxue. 2022. Heavy mineral assemblages and migration paths in the surface sediments of the northern East China Sea shelf: tracer responses to bottom water masses. Earth Science Frontiers (in Chinese), 29(5): 88–101

Liu Jian, Li Shaoquan, Wang Shengjie, et al. 1999. Sea level changes of the Yellow Sea and formation of the Yellow Sea warm current since the last deglaciation. Marine Geology & Quaternary Geology (in Chinese), 19(1): 13–24

Liu Shengfa, Liu Yanguang, Zhu Aimei, et al. 2009. Grain size trends and net transport patterns of surface sediments in the East China Sea inner continental shelf. Marine Geology & Quaternary Geology (in Chinese), 29(1): 1–6

J.Paul Liu, Milliman J D, Gao Shu, et al. 2004. Holocene development of the Yellow River's subaqueous delta, North Yellow Sea. Marine Geology, 209(1–4): 45–67, doi: 10.1016/j.margeo.2004.06.009

Liu Tao, Shi Xuefa, Liu Yanguang, et al. 2014. Diffusion of sediment in radial sand ridges in southern Yellow Sea. Oceanologia et Limnologia Sinica (in Chinese), 45(1): 32–38

Liu Zhifei, Trentesaux A, Clemens S C, et al. 2003. Clay mineral assemblages in the northern South China Sea: implications for East Asian monsoon evolution over the past 2 million years. Marine Geology, 201(1–3): 133–146, doi: 10.1016/S0025-3227(03)00213-5

Liu Zhenxia, Xia Dongxing. 2004. Tidal Sands in the China Seas (in Chinese). Beijing: China Ocean Press, 222

Liu Zhifei, Zhao Yulong, Li Jianru, et al. 2007. Late Quaternary clay minerals off Middle Vietnam in the western South China Sea: implications for source analysis and East Asian monsoon evolution. Science in China Series D: Earth Sciences, 50(11): 1674–1684, doi: 10.1007/s11430-007-0115-8

Lu Jian, Li Anchun, Zhang Jin, et al. 2019. Yangtze River-derived sediments in the southwestern South Yellow Sea: provenance discrimination and seasonal transport mechanisms. Journal of Asian Earth Sciences, 176: 353–367, doi: 10.1016/j.jseaes.2019.03.007

Lupker M, France-Lanord C, Galy V, et al. 2013. Increasing chemical weathering in the Himalayan system since the Last Glacial Maximum. Earth and Planetary Science Letters, 365: 243–252, doi: 10.1016/j.epsl.2013.01.038

McLaren P, Bowles D. 1985. The effects of sediment transport on grain-size distributions. Journal of Sedimentary Research, 55(4): 457–470

Milliman J D, Beardsley R C, Yang Zuosheng, et al. 1985. Modern Huanghe-derived muds on the outer shelf of the East China Sea: identification and potential transport mechanisms. Continental Shelf Research, 4(1–2): 175–188, doi: 10.1016/0278-4343(85)90028-7

Ning Ze, Xu Lei, Lin Xuehui, et al. 2022. Distribution and provenance of detrital minerals in surface sediments of the northeastern East China Sea. Marine Geology & Quaternary Geology (in Chinese), 42(5): 58–69

Niu Zuomin. 1985. Deposition environment sub-division of the East China Sea and their basic features. Marine Geology & Quaternary Geology (in Chinese), 5(2): 27–36

Park Y A, Khim B K. 1992. Origin and dispersal of recent clay minerals in the Yellow Sea. Marine Geology, 104(1–4): 205–213, doi: 10.1016/0025-3227(92)90095-Y

Qiao Shuqing, Yang Zuosheng. 2007. Comparison of rare earth element compositions in different grain-size fractions of sediments from the Yangtze and Yellow Rivers and the Sea. Marine Geology & Quaternary Geology (in Chinese), 27(6): 9–16

Qin Yunshan, Zhao Yiyang, Chen Lirong, et al. 1987. Geology of the East China Sea (in Chinese). Beijing: Science Press

Rao Wenbo, Mao Changping, Wang Yigang, et al. 2017. Using Nd-Sr isotopes and rare earth elements to study sediment provenance of the modern radial sand ridges in the southwestern Yellow Sea. Applied Geochemistry, 81: 23–35, doi: 10.1016/j.apgeochem.2017.03.011

Ren Meie, Shi Yunliang. 1986. Sediment discharge of the Yellow River and its effect on sedimentation of the Bohai and Yellow Sea. Scientia Geographica Sinica (in Chinese), 6(1): 1–12,101

Shi Xuefa. 2012. The Oceanic Substrate of China's Offshore (in Chinese). Beijing: China Ocean Press, 561

Shi Xuefa. 2021. Sediment Type Map of the Bohai Sea, Yellow Sea and East China Sea (in Chinese). Beijing: China Science Press, 116

Shi Yong, Gao Jianhua, Liu Qiang, et al. 2019. Fine sediment transport in north-central of Yellow Sea: the role of continental shelf circulation. Haiyang Xuebao (in Chinese), 41(4): 53–63

Song Y H, Choi M S. 2009. REE geochemistry of fine-grained sediments from major rivers around the Yellow Sea. Chemical Geology, 266(3–4): 328–342, doi: 10.1016/j.chemgeo.2009.06.019

Sun Xiaogong, Fang Ming, Huang Wei. 2000. Spatial and temporal variations in suspended particulate matter transport on the Yellow and East China Sea shelf. Oceanologia et Limnologia Sinica (in Chinese), 31(6): 581–587

McLennans S M. 2001. Relationships between the trace element composition of sedimentary rocks and upper continental crust. Geochemistry, Geophysics, Geosystems, 2(4): 2000GC000109, doi: 10.1029/2000GC000109

Wang Liang. 2014. High-resolution sedimentary record in the typical mud areas of East China Sea and its response to climate and environmental changes (in Chinese)[dissertation]. Qingdao: Ocean University of China

Wang Zhongbo, Lu Kai, Wen Zhenhe, et al. 2020. Grain size compositions and their influencing factors of the surface sediments in eastern China Seas. Earth Science (in Chinese), 45(7): 2709–2721

Wang Guoqing, Shi Xuefa, Liu Yanguang, et al. 2007. Study on geochemical province of bottom sediment elements from south branch of the Changjiang River estuary. Advances in Marine Science (in Chinese), 25(4): 408–418

Wang Zhongbo, Yang Shouye, Zhang Zhixun, et al. 2012a. The grain size compositions of the surface sediments in the East China Sea: indication for sedimentary environments. Oceanologia et Limnologia Sinica (in Chinese), 43(6): 1039–1049

Wang Zhongbo, Yang Shouye, Zhang Zhixun, et al. 2012b. A review of the late quaternary sedimentological studies on the outer shelf of the East China Sea. Marine Geology & Quaternary Geology (in Chinese), 32(3): 1–10

Xiong Yingqian, Yang Zuosheng, Liu Zhenxia. 2003. A review of source study of the Changjiang and Yellow River sediments. Advances in Marine Science (in Chinese), 21(3): 355–362

Xu Zhaokai, Lim D, Choi J, et al. 2009a. Rare earth elements in bottom sediments of major rivers around the Yellow Sea: implications for sediment provenance. Geo-Marine Letters, 29(5): 291–300., doi: 10.1007/s00367-009-0142-x

Xu Kehui, Milliman J D, Li Anchun, et al. 2009b. Yangtze- and Taiwan-derived sediments on the inner shelf of East China Sea. Continental Shelf Research, 29(18): 2240–2256, doi: 10.1016/j.

csr.2009.08.017
Yang Zuosheng. 1988. Mineralogical assemblages and chemical characteristics of clays from sediments of the Huanghe, Changjiang, Zhujiang Rivers and their relationship to the climate environment in their sediment source areas. Oceanologia et Limnologia Sinica (in Chinese), 19(4): 336–346
Yang Shouye, Jung H S, Choi M S, et al. 2002. The rare earth element compositions of the Changjiang (Yangtze) and Huanghe (Yellow) river sediments. Earth and Planetary Science Letters, 201(2): 407–419, doi: 10.1016/S0012-821X(02)00715-X
Yang Shouye, Jung H S, Lim D I, et al. 2003a. A review on the provenance discrimination of sediments in the Yellow Sea. Earth-Science Reviews, 63(1–2): 93–120, doi: 10.1016/S0012-8252(03)00033-3
Yang Shouye, Li Congxian. 1999a. REE geochemistry and tracing applicationin the Yangtze River and the Yellow River sediments. Geochimica (in Chinese), 28(4): 374–380
Yang Shouye, Li Congxian. 1999b. Characteristic element compositions of the Yangtze and the Yellow River sediments and their geological background. Marine Geology & Quaternary Geology (in Chinese), 19(2): 19–26
Yang Shouye, Li Congxian, Jung H S, et al. 2003b. Geochemistry of trace elements in Chinese and Korean river sediments. Marine Geology & Quaternary Geology (in Chinese), 23(2): 19–24
Yang Shouye, Lim D I, Jung H S, et al. 2004. Geochemical composition and provenance discrimination of coastal sediments around Cheju Island in the southeastern Yellow Sea. Marine Geology, 206(1–4): 41–53, doi: 10.1016/j.margeo.2004.01.005
Yang Zigeng, Wang Shengjie, Zhang Guangwei, et al. 2001. Evolution model for south Yellow Sea tidal sand ridges during transgressions in deglaciation. Marine Geology & Quaternary Geology (in Chinese), 21(3): 1–10
Ye Yincan, Zhuang Zhenye, Lai Xianghua, et al. 2004. A study of sandy bedforms on the Yangtze Shoal in the East China Sea. Periodical of Ocean University of China (in Chinese), 34(6): 1057–1062
Yin Ping. 2003. Geomorphology and internal structure of postglacial tidal sand ridges on the East China Sea shelf. Advances in Marine Science (in Chinese), 21(2): 181–187
Youn J S. 2009. Clay minerals and geochemistry of continental shelf sediment around Jeju Island in the northern East China Sea. The Korean Journal of Quaternary Research (in Korean), 23(1): 25–37
Youn J S, Byun J C, Kim Y S. 2006. Geochemical characteristics of the outer-shelf muddy sediments in the East China Sea. Journal of the Korean Earth Science Society (in Korean), 27(2): 198–208
Youn J, Kim T J. 2011. Geochemical composition and provenance of muddy shelf deposits in the East China Sea. Quaternary International, 230(1–2): 3–12, doi: 10.1016/j.quaint.2009.11.001
Zhang Zhixin. 2014. Observation and analysis of the coastal current and its adjacent current system in the China offshore waters (in Chinese)[dissertation]. Qingdao: Ocean University of China
Zhang Jing, Huang Weiwen, Liu Minguang, et al. 1990. Drainage basin weathering and major element transport of two large Chinese rivers (Huanghe and Changjiang). Journal of Geophysical Research: Oceans, 95(C8): 13277–13288, doi: 10.1029/JC095iC08p13277
Zhang Kaidi, Li Anchun, Dong Jiang, et al. 2016. Detrital mineral distributions in surface sediments of the East China Sea: implications for sediment provenance and sedimentary environment. Acta Sedimentologica Sinica (in Chinese), 34(5): 902–911
Zhao Li, Cai Guanqiang, Zhong Hexian, et al. 2021. Grain size distribution of surface sediments in the area off southeast Hainan Island and its implications for environmental interpretation. Marine Geology & Quaternary Geology (in Chinese), 41(2): 64–74
Zhao Yiyang, Yan Mingcai. 1994. Geochemistry of Sediments of the China Shelf Sea (in Chinese). Beijing: Science Press, 203
Zhao Yiyang, Zhang Xiulian, Xia Qing, et al. 1986. Chemical characteristics of various sediments in the East China Sea. Chinese Science Bulletin (in Chinese), 31(20): 1573–1575, doi: 10.1360/csb1986-31-20-1573
Zhou Huaiyang, Ye Ying, Shen Zhongyue. 2004. On the variation of clay minerals and their paleosedimentary records in the sediment cores in the southern area of the South China Sea. Haiyang Xuebao (in Chinese), 26(2): 52–60
Zhu Yingtao, Bao Rui, Zhu Longhai, et al. 2022. Investigating the provenances and transport mechanisms of surface sediments in the offshore muddy area of Shandong Peninsula: insights from REE analyses. Journal of Marine Systems, 226: 103671, doi: 10.1016/j.jmarsys.2021.103671
Zhu Jianrong, Shen Huanting. 1997. The Mechanism of the Expansion of the Changjiang (Yangtze River) Diluted Water (in Chinese). Shanghai: East China Normal University Press, 255
Zhu Erqin, Wang Qi, Li Jianhua, et al. 1986. Formation of carbonate in the surface sediments in the northern part of the East China Sea. Acta Sedimentologica Sinica (in Chinese), 4(3): 43–56
Zhu Jianrong, Xiao Chengyou, Shen Huanting. 1998. Numerical model simulation of expansion of Changjiang diluted water in summer. Haiyang Xuebao (in Chinese), 20(5): 13–22